NUREG/CR-6524
BNL-NUREG-52518

The Effect of Lateral Venting on Deflagration-to-Detonation Transition in Hydrogen-Air-Steam Mixtures at Various Initial Temperatures

Prepared by
G. Ciccarelli, J. L. Boccio, T. Ginsberg, C. Finfrock, L. Gerlach/ BNL
H. Tagawa/ NUPEC
A. Malliakos/NRC

Brookhaven National Laboratory

Prepared for
U. S. Nuclear Regulatory Commission

and

Nuclear Power Engineering Corporation

AVAILABILITY NOTICE

Availability of Reference Materials Cited in NRC Publications

NRC publications in the NUREG series, NRC regulations, and *Title 10, Energy,* of the *Code of Federal Regulations,* may be purchased from one of the following sources:

1. The Superintendent of Documents
   U.S. Government Printing Office
   P.O. Box 37082
   Washington, DC 20402–9328
   <http://www.access.gpo.gov/su_docs>
   202–512–1800

2. The National Technical Information Service
   Springfield, VA 22161–0002
   <http://www.ntis.gov/ordernow>
   703–487–4650

The NUREG series comprises (1) technical and administrative reports, including those prepared for international agreements, (2) brochures, (3) proceedings of conferences and workshops, (4) adjudications and other issuances of the Commission and Atomic Safety and Licensing Boards, and (5) books.

A single copy of each NRC draft report is available free, to the extent of supply, upon written request as follows:

Address: Office of the Chief Information Officer
Reproduction and Distribution
Services Section
U.S. Nuclear Regulatory Commission
Washington, DC 20555–0001
E–mail: <GRW1@NRC.GOV>
Facsimile: 301–415–2289

A portion of NRC regulatory and technical information is available at NRC's World Wide Web site:

<http://www.nrc.gov>

All NRC documents released to the public are available for inspection or copying for a fee, in paper, microfiche, or, in some cases, diskette, from the Public Document Room (PDR):

NRC Public Document Room
2121 L Street, N.W., Lower Level
Washington, DC 20555–0001
<http://www.nrc.gov/NRC/PDR/pdr1.htm>
1–800–397–4209 or locally 202–634–3273

Microfiche of most NRC documents made publicly available since January 1981 may be found in the Local Public Document Rooms (LPDRs) located in the vicinity of nuclear power plants. The locations of the LPDRs may be obtained from the PDR (see previous paragraph) or through:

<http://www.nrc.gov/NRC/NUREGS/SR1350/V9/lpdr/html>

Publicly released documents include, to name a few, NUREG-series reports; *Federal Register* notices; applicant, licensee, and vendor documents and correspondence; NRC correspondence and internal memoranda; bulletins and information notices; inspection and investigation reports; licensee event reports; and Commission papers and their attachments.

Documents available from public and special technical libraries include all open literature items, such as books, journal articles, and transactions, *Federal Register* notices, Federal and State legislation, and congressional reports. Such documents as theses, dissertations, foreign reports and translations, and non-NRC conference proceedings may be purchased from their sponsoring organization.

Copies of industry codes and standards used in a substantive manner in the NRC regulatory process are maintained at the NRC Library, Two White Flint North, 11545 Rockville Pike, Rockville, MD 20852–2738. These standards are available in the library for reference use by the public. Codes and standards are usually copyrighted and may be purchased from the originating organization or, if they are American National Standards, from—

American National Standards Institute
11 West 42nd Street
New York, NY 10036–8002
<http://www.ansi.org>
212–642–4900

NUREG/CR-6524
BNL-NUREG-52518

The Effect of Lateral Venting on Deflagration-to-Detonation Transition in Hydrogen-Air-Steam Mixtures at Various Initial Temperatures

Manuscript Completed: July 1998
Date Published: November 1998

Prepared by
G. Ciccarelli, J. L. Boccio, T. Ginsberg, C. Finfrock, L. Gerlach/BNL
H. Tagawa/NUPEC
A. Malliakos/NRC

Brookhaven National Laboratory
Upton, NY 11973-5000

A. Malliakos, NRC Project Manager

Prepared for
Division of Systems Technology
Office of Nuclear Regulatory Research
U.S. Nuclear Regulatory Commission
Washington, DC 20555-0001
NRC Job Code L1924/A3991

and

Nuclear Power Engineering Corporation
5F Fujita Kanko Toranomon Building
3-17-1, Toranomon, Minato-Ku
Tokyo 105
Japan

NUREG/CR-6524 has been reproduced from the best copy available.

ABSTRACT

The influence of gas venting on flame acceleration in an obstacle-laden tube has been investigated in the High-Temperature Combustion Facility (HTCF) at BNL. The main component of the HTCF is a 27.3-cm- inner diameter heated detonation tube. In the present experiments, five 3.1-meter-long tube sections were used with a vent section placed in between each tube section. The total vent area per vent section is four times the tube's cross-sectional area. The entire length of the vessel is filled with 20.6-cm-inner diameter orifice plates, with 27.3-cm spacing, to promote flame acceleration. Hydrogen-air-steam mixtures were tested at initial temperatures up to 650K and at an initial pressure of 0.1 MPa.

In these venting experiments, the flame was observed to accelerate very quickly in the first tube section before the first vent section. For lean hydrogen mixtures, after the first vent section, the flame velocity decayed to a velocity on the order of the laminar burning velocity. For more sensitive mixtures, the flame reached a quasi-steady flame velocity similar to flame propagation in the choking regime observed in tests without venting. For all initial temperatures, the lean limit for significant flame acceleration (i.e., choking regime limit) with venting increased over the nonventing case by an average of 2 percent hydrogen. In the choking regime, the flame was observed to accelerate in the tube section to a maximum velocity close to the speed of sound in the products and then decelerate across the vent section. There was little evidence of any variation in the global average velocity (i.e., average over the length of one vent and tube section) once the flame entered this mode of propagation. Pressure measurements taken before the last vent section, near the end of the tube, were similar to overpressures measured in tests without venting. At the limited temperatures tested where DDT was observed, the minimum hydrogen concentration required for transition to detonation increased with venting present as compared to without venting. In all cases, after a certain propagation distance, the detonation wave failed due to local venting effects and continued to propagate at a velocity characteristic of the choking regime.

TABLE OF CONTENTS

LIST OF FIGURES

EXECUTIVE SUMMARY

This report deals with the effects of gas venting on flame acceleration and deflagration-to-detonation transition (DDT) phenomenon. This report can be considered a companion to NUREG/CR-6509 which dealt with the same phenomenon without venting. These two test series, along with an initial series of experiments measuring the detonation cell size, are part of the High-Temperature Hydrogen Combustion Research Program, which is jointly funded by the U.S. Nuclear Regulatory Commission and the Japanese Nuclear Power Engineering Corporation, which is sponsored by the Ministry of International Trade and Industry (MITI). The objective of the program is to study high-speed combustion phenomena in hydrogen-air-steam mixtures at high initial temperatures, which may be produced in a nuclear power plant during a severe-accident scenario. The High-Temperature Combustion Facility (HTCF) was constructed at Brookhaven National Laboratory with the unique capability of studying high-temperature detonation phenomenon.

One of the concerns during a severe accident in a water-cooled nuclear reactor is the accumulation in the containment and subsequent combustion of hydrogen generated in the core as a result of water-metal reactions. Of special concern is the possibility of the initiation of a detonation wave which has the potential to damage the containment structure. The most probable mode of detonation initiation is through flame acceleration and transition to detonation. In a nuclear power plant, flame acceleration is most likely to occur in long narrow rooms, or corridors, containing equipment or other type of obstructions that could promote turbulence of the gaseous mixture within the confining geometry. In such realistic geometries, doorways and other openings can provide venting pathways for burnt gases that can hinder the flame acceleration process.

The HTCF consists of a detonation tube which can be heated to a maximum temperature of 700K with a temperature uniformity of ±14K. The detonation tube is 21.3-meters long and is constructed from sections of stainless steel pipe with an internal diameter of 27.3 cm. Instrumentation ports are located at regular intervals of 0.61 meters. The test gases are mixed in a chamber fed by two pipes: one flowing air at room temperature and the other a heated mixture of hydrogen and steam. The desired mixture composition is achieved by varying the individual constituent flow rates via choked venturis. In the experiments looking at DDT phenomenon, a flame is ignited which subsequently accelerates as a result of turbulence generated in the induced flow ahead of the flame. For certain mixtures, this flame acceleration could lead to the initiation of a detonation wave. In order to promote flame acceleration, periodic orifice plates were installed down the length of the entire detonation tube. The orifice plates have an outer diameter of 27.3 cm (equivalent to the inner diameter of the tube), an inner diameter of 20.6 cm, and have a spacing of one tube diameter. A standard automobile diesel engine glow plug is used to ignite the test mixture at one end of the tube.

For these venting experiments, the main modification to the detonation vessel was the addition of four vent sections which were inserted between nonvented pipe sections. These vent sections consist of two standard pipe-crosses butt welded together, each pipe-cross having the same inner diameter as the detonation tube. The total vent area per vent section is thus four times the detonation tube cross-section area. The vent openings are initially closed by vent covers which are dislodged when the vessel pressure increases as a result of combustion. The welded pipe-crosses are mated to the straight pipe section using compatible flanges. The length of a vent section is 1.52 meters which is exactly half the length of a standard HTCF straight pipe section. In order to maintain the same total vessel length to diameter ratio (e.g., 78) as the vessel without the vent sections, two of the straight sections are not utilized in the present experiments. In this way, five straight pipe sections are separated from each other by one of the four vent sections.

The parameters which most influence the flame acceleration process are the mixture composition, which includes the hydrogen concentration and the steam dilution, and the mixture initial temperature. The hydrogen concentration was varied from a minimum where benign flames were produced to a

maximum where vent covers were dislodged from their tethers. The initial temperature was varied between 300K and 650K, and the initial pressure was 0.1 MPa for all tests.

In general, for the test apparatus configuration studied, venting reduced the likelihood of DDT at all initial temperatures tested. Flame propagation in the vented tube geometry consists of an initial flame acceleration phase followed by a quasi-steady-state phase where the combustion front velocity oscillates about a mean. The various flame propagation regimes have been classified as: (1) slow deflagrations, (2) choking, and (3) detonation. The flame propagation in these various regimes is qualitatively similar to that observed in the tests without venting, except for local perturbations induced by the vent sections. In the slow deflagration regime, the flame accelerates to a maximum velocity of about 100-200 m/s around the first vent section and then for the remainder of the tube decelerates to a velocity on the order of meters per second. No significant pressure is generated in this propagation regime.

In the choking regime, flame acceleration is followed by an oscillatory propagation mode where the flame accelerates in the tube section and decelerates across the vent section. The mean flame velocity during the oscillatory propagation is just under the speed of sound in the burnt products. The structure of the combustion front consists of a turbulent flame preceded by a weak precursor shock wave and a stronger leading shock wave. The leading shock wave is generated as a result of the coalescing of compression waves generated ahead of the turbulent flame. This leading shock wave has a typical pressure rise just under the Adiabatic Isochoric Complete Combustion (AICC) pressure. The weak wave is generated by the decoupling of the leading shock wave and the flame during their passage through the vent section. Therefore, the weak precursor wave is a product of the leading shock wave after it emerges from the vent section.

In the detonation propagation regime, which exists for particularly sensitive mixtures, a detonation wave is initiated at some point during flame acceleration. In all the cases tested, the detonation wave failed before the end of the vessel as a result of wave diffraction in the vent section. However, one would expect if the mixture cell size is small enough, a detonation wave could propagate through the entire vessel unimpeded by the orifice plates and the venting.

The influence of venting on the combustion phenomenon could be measured by the magnitude of change in the choking and the DDT limits from tests without venting to tests with venting. The choking limit, which is in effect the minimum hydrogen composition where significant flame acceleration takes place, increased for all initial temperatures and steam dilution in the experiments with venting. The DDT limit, which in this case is defined as the minimum hydrogen composition where a detonation is observed, was equally affected by venting. For example, for hydrogen-air mixtures at 500K the DDT limits increased from 12 percent hydrogen with no venting to 15 percent hydrogen with venting. The study without venting had shown that for hydrogen-air mixtures at 500K the DDT limit criterion was $d/\lambda = 1$. In the present study with venting, for hydrogen-air mixtures at 500K, the DDT limit is $d/\lambda = 5.5$.

At the present time, the only quantitative method for determining the possibility for transition to detonation in a given compartment is by using the $d/\lambda = 1$ DDT limit criterion derived from experiments in obstacle-laden tubes. This criterion states that only those mixtures whose detonation cell size is smaller than the length scale of the compartment in question may result in a detonation. This criterion does not take into account the shape of the compartments or any possible vent openings. The experiments presented here have shown that venting has a mitigating effect on transition to detonation, and thus, the above criterion has a built-in safety margin.

ACKNOWLEDGMENTS

The authors would like to acknowledge the technical guidance provided by Dr. John Lee of McGill University and Dr. Joseph Shepherd of the California Institute of Technology. We have frequently drawn upon their experience in the field of detonation physics and gained from many fruitful discussions.

We would also like to acknowledge the review of the report by Dr. Hideo Ogasawara and Mr. Takashi Hashimoto of the Nuclear Power Engineering Corporation, Tokyo, Japan.

This study was performed within the Safety and Risk Evaluation Division of the Department of Advanced Technology, Brookhaven National Laboratory. The administrative support of Dr. W. T. Pratt, Division Head, and Dr. R. A. Bari, Department Head, are much appreciated.

The authors would like to thank Ms. Jean Frejka for her continued assistance in the administrative aspects of the project and for her help in the preparation of this report.

1. INTRODUCTION

During a postulated severe accident in a light-water nuclear reactor, hydrogen is produced in the reactor core primarily as a result of the reaction between the zirconium metal cladding and the steam in the degraded core. The hydrogen, along with considerable amounts of steam, eventually find their way into various containment compartments where they can mix with preexisting air. The possibility of initiation of a detonation wave in this combustible mixture could pose a threat to the integrity of the containment building. Direct initiation of a spherical detonation requires a considerable amount of energy to be deposited in the combustible mixture in a very short time (Guirao et al., 1989). It is generally acknowledged that direct initiation of a detonation is a highly unlikely event in a nuclear power plant environment considering the large critical energies associated with the insensitive hydrogen-air-steam mixtures predicted to exist during such an accident. A more plausible scenario for detonation initiation is via flame acceleration or hot jet initiation. This report deals exclusively with detonation initiation resulting from flame acceleration, commonly referred to as Deflagration-to-Detonation Transition (DDT), and the influence of gas venting on this phenomenon.

In a nuclear power plant, flame acceleration is most likely to occur in long narrow rooms, or corridors, containing equipment or other type of obstructions that could promote turbulence in the induced gas flow ahead of the flame. In such realistic geometries, doorways and other openings can provide venting pathways for the burnt gas that can hinder the flame acceleration process. Due to the common use of explosion venting devices in the chemical industry, extensive efforts have gone into the study of venting of explosions in confined volumes. Guidelines have been established by the National Fire Protection Association for the venting of deflagrations (NFPA 68). However, the bulk of the experimental and theoretical work on the subject pertains to enclosures which have a length to diameter ratio of less than 3 where flame acceleration is very limited. Also, the test mixtures used in these investigations are typically associated with the chemical and pipeline industry (e.g., propane and methane), which are considerably less sensitive than hydrogen-air mixtures.

Flame acceleration occurs more aptly in enclosures having large length-to-diameter ratios. In such a geometry, flame acceleration is due to a feedback mechanism between the burning rate of the flame and the induced flow ahead of the flame. A flow is generated ahead of the flame due to the expansion of the high-temperature combustion products. In a duct there is no divergence of the flow and the duct boundary provides a source of vorticity which is necessary to achieve very high flame velocities required for DDT. The presence of obstacles in a 1-dimensional geometry produces flow disturbances which greatly enhances the flame acceleration process. Historically, flame acceleration leading to the onset of detonation has been studied in long pipes with, or without, obstacles (Guirao et al., 1986; Beauvais et al., 1993; and Ciccarelli et al., 1996). In this study, a vented obstacle-laden cylindrical tube, with a length to diameter ratio of 78, is used to study the effects of venting on DDT. The experimental device is part of the High-Temperature Combustion Facility (HTCF) located at Brookhaven National Laboratory, depicted in Figure 1.1.

The High-Temperature Hydrogen Combustion Research Program at Brookhaven National Laboratory is a jointly funded program by the U.S. Nuclear Regulatory Commission and the Japanese Nuclear Power Engineering Corporation, which is sponsored by the Ministry of International Trade and Industry (MITI). The overall objective of the program is to develop a data base which can be used to assess hydrogen combustion phenomena in mixtures of hydrogen, air and steam at high temperature. Results obtained in the first element of the program, focussing on measurement of detonation cell size, were reported in NUREG/CR-6213 and NUREG/CR-6391. Results on the effect of initial temperature on nonvented DDT phenomenon in hydrogen-air and steam mixtures are reported in NUREG/CR-6509. This report

summarizes the results from the investigation of the influence of venting on flame acceleration and DDT phenomenon in hydrogen-air-steam mixtures at various initial temperatures and could be considered a companion document to NUREG/CR-6509.

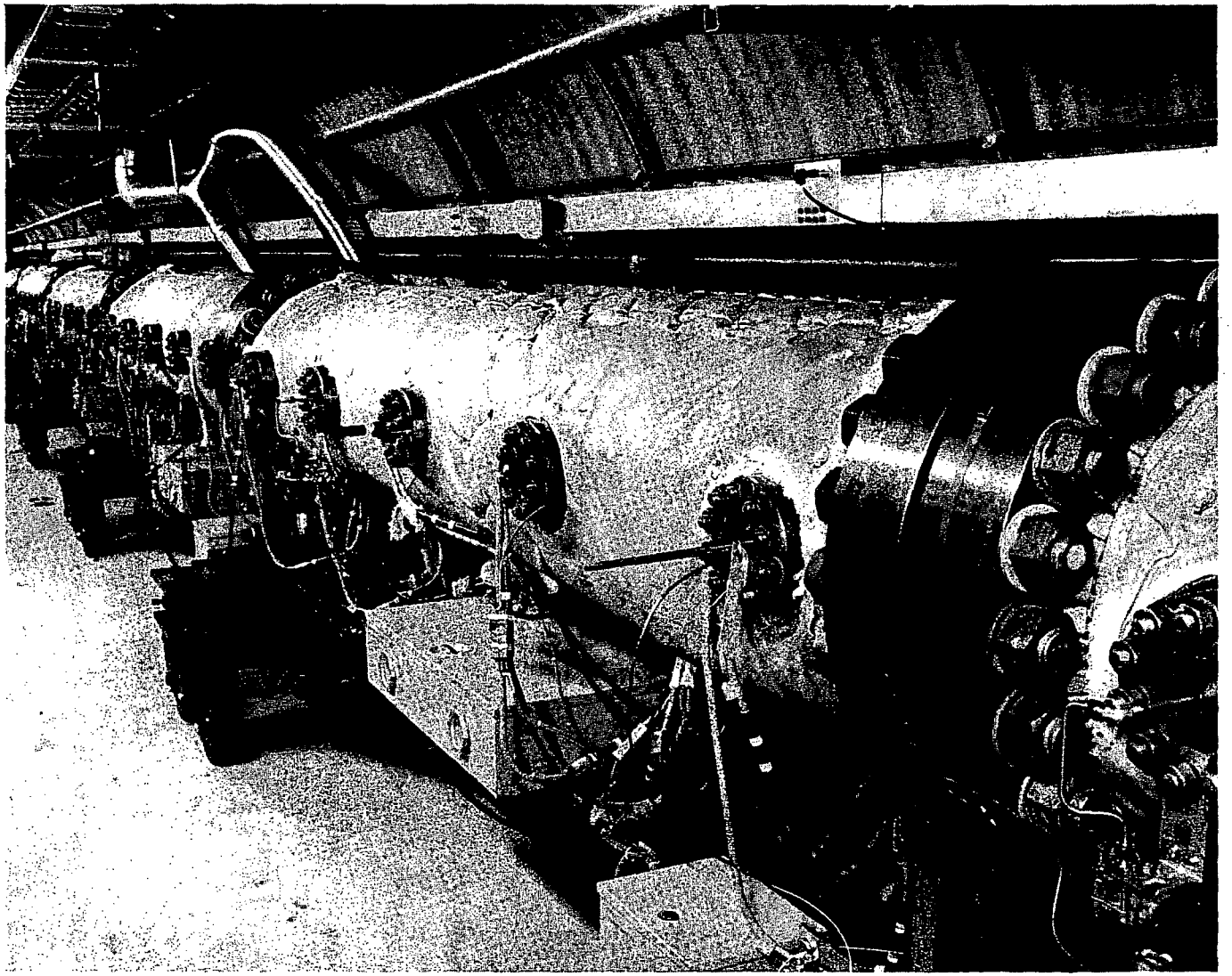

Figure 1.1 Photograph of the detonation tube located inside the 3.05-meter tunnel

2. BACKGROUND

The following two sections provide some background information on flame acceleration and explosion venting. A more detailed discussion on flame acceleration and related DDT phenomenon can be found in NUREG/CR-6509.

2.1 Flame Acceleration and DDT With No Venting

If a combustible mixture is confined in a relatively long narrow duct and a flame is ignited at one of the closed ends, it will accelerate as a result of the turbulent flow generated ahead of the flame. The flow ahead of the flame is produced as a result of the increase in the gas specific volume across the flame. As the flame accelerates, it generates compression waves ahead of it which eventually coalesce to form a leading shock wave. In relatively sensitive mixtures, this flame acceleration and shock formation can lead to transition to detonation. If turbulence-inducing obstacles (e.g., orifice plates) are placed in the duct, the rate of flame acceleration will be significantly increased along with the possibility for DDT. In experiments carried out in long tubes filled with orifice plates, the flame is observed to accelerate to a final steady-state velocity (Guirao et al., 1989 and Ciccarelli et al., 1996).

The combustion front propagation mode during this final steady-state phase has been classified as the "choking" and "quasi-detonation" regimes. In the choking regime, the combustion front propagates at a velocity equal to the isobaric speed of sound in the combustion products. In this mode of combustion, the flame supports a precursor shock wave that moves at a velocity slightly higher than the flame. Therefore, the flame and the precursor shock wave are not intimately coupled as is the case in a detonation wave where the leading shock wave initiates the exothermic chemical reactions in the mixture. In the quasi-detonation regime, flame acceleration leads to the onset of detonation, and, therefore, this mode of propagation consists of a detonation wave which propagates at a velocity below the theoretical CJ detonation velocity. This velocity deficit is due to severe momentum and heat losses from the reaction zone to the orifice plates. The absolute amount of velocity deficit relative to the theoretical CJ detonation velocity depends on the reaction zone length which increases with decreasing hydrogen concentration below stoichiometric.

It has been shown, in general, that the minimum hydrogen concentration required for transition to detonation corresponds to the mixture whose detonation cell size, λ, is equal to the orifice plate inner diameter, d (e.g., $d/\lambda = 1$). Therefore, DDT can occur for hydrogen-air mixtures whose detonation cell size is smaller than the orifice plate diameter. For hydrogen-air mixtures at 650K, the leanest hydrogen-air mixture resulting in DDT corresponded to a value of $d/\lambda = 5.5$ (Ciccarelli et al., 1996). This apparent variance in the DDT limit criterion, in these high-temperature mixtures, is due to the inability of the flame to accelerate to a point where the conditions within the flame-shock complex are conducive to the initiation of a detonation. Therefore, at elevated temperatures, the $d/\lambda = 1$ limit criteria provides a necessary but not sufficient condition for DDT.

2.2 Flame Acceleration and DDT With Venting

The maximum pressure achievable in a closed volume by a deflagration is the Adiabatic Isochoric Complete Combustion (AICC) pressure which for most combustible gases near stoichiometric conditions is typically in the range of six to eight times the initial pressure. It is very costly to design structures which can withstand such pressures, and, therefore, pressure relief devices are commonly used to limit the degree of pressurization to a level below the design strength of the enclosure. In the chemical

industry, the enclosures of interest typically have small length-to-width ratios (e.g., buildings, rooms, ovens, tanks, etc.). As a result, most of the existing data in the literature on explosion venting was obtained from spherical vessels equipped with one venting device (Bradley and Mitcheson, 1978). In these tests, the maximum measured enclosure pressure is measured for a given combustible mixture, enclosure volume, and vent area. This data can then be correlated and presented in graphical form, or as a simple empirical relation giving the required vent area as a function of the enclosure volume, the enclosure design pressure, and several constants whose values depend on the test mixture.

In these types of experiments, no turbulence is generated in the flow ahead of the flame since the flow is symmetric, and no velocity gradients are present at the enclosure boundary. The effect of turbulence can be studied by artificially generating turbulence inside the enclosure (e.g., by a fan) before ignition. An increase in the burning rate can also occur naturally as a result of flame instabilities that are generated by interactions between the flame and acoustic reverberations in the enclosure (Cooper et al., 1986) or by the sudden acceleration of the flame when the products are vented from the enclosure (Solberg and Pappas, 1981).

Most of the studies examining venting in large length/diameter (L/D) vessels are performed in ducts with a single vent located at the end of the vessel opposite the ignition end. One of the first studies into the venting of explosions in long ducts was carried out by Rabash and Rogowski (1960). In their investigation, they measured the peak pressure and flame velocity in pentane and propane-air mixtures. They varied the vent opening area and the duct diameter. They found that the measured vessel overpressure decreased linearly with increased vent area and that the maximum flame velocity increased with increasing venting area. These findings have recently been confirmed by Tite et al. (1991) and Alexiou et al. (1995). These findings can be explained by the fact that an increase in the vent area results in a larger vent mass flow rate which results in a slower vessel pressurization rate. Therefore, in the time it takes the flame to propagate the length of the vessel, more mass is ejected from the vent opening, resulting in a lower peak pressure. The larger vent mass flow rate also results in a higher mean flow velocity ahead of the flame. This directly increases the flame velocity since the flame is convected by the mean flow of the unburnt gas and indirectly increases the flame velocity by increasing the turbulence intensity in the flow ahead of the flame.

When a flame propagates down a long duct with a vent located at the end opposite the ignition source, there are actually three pressure peaks detected in the vessel (Alexiou et al., 1995). The initial pressure rise is a result of the volumetric burning rate being higher than the volumetric venting rate of the unburnt gas. In this initial phase, the flame takes on a parabolic shape which elongates with time. The increased flame surface area associated with the flame elongation leads to an increase in the overall burning rate. Once the flame reaches the side wall of the duct, the reduced flame surface area results in a reduced volumetric burning rate resulting in a drop in pressure. As the turbulence intensity in the flow ahead of the flame increases, the flame reaccelerates, and the pressure rises. Once the flame reaches the vent, the pressure drops as a result of the high volumetric burnt gas flow through the vent. The third peak in pressure is due to the rapid combustion of the unburnt gas downstream of the vent in the dump tank. In these types of tests in smooth tubes using methane or propane-air mixtures, the maximum flame velocity achieved is only about 100 to 150 m/s.

The influence of turbulence producing devices, such as valves, on increasing the effective burning rate of the flame has been recognized for a long time. Recently, Alexiou et al. (1995) have investigated the effect of a single orifice placed in an otherwise smooth tube with a fully open vent at the end of

the tube. They found that the same three pressure peaks exist, as when no obstacle is present, only the second peak was significantly larger. This was attributed to the increase in the turbulence in the unburnt gas downstream of the orifice. The magnitude of the pressure peak was observed to increase with increasing blockage. With the orifice plate in place, the rate of pressure rise of the second peak increased with blockage ratio to a maximum of about 25 times the rate with no orifice plate. They also showed empirically that the turbulent burning velocity downstream of the orifice was 131 times the laminar burning velocity in the same mixture and 17 times the turbulent burning velocity if no obstacle was present.

A study on the effect of venting on flame acceleration in hydrogen-air mixtures in vessels with repeated obstacles was performed at Sandia National Laboratory (SNL) in the FLAME Facility (Sherman et al., 1989). The FLAME Facility is a 30.5-meter-long concrete channel which is 1.83-meters high and 2.44-meters wide (e.g., length-to-average width ratio of 14.3). Flame acceleration was promoted using plywood baffles placed on either side of the channel, yielding a blockage of 33 percent. The top of the channel consists of 38.5-cm-thick reinforced steel plates. Tests were run with all the plates in place (0 percent top venting), with every other plate installed (50 percent top venting) and with the plates partially separated (13 percent top venting). The ignition end was closed and the opposite end was open. Both pressure measurements and flame time-of-arrival measurements were made.

In the FLAME Facility, tests were performed with hydrogen-air mixtures containing 12 to 30 percent hydrogen at an initial temperature of 300K. Without obstacles and no venting, no flame acceleration was observed for mixtures below 13 percent hydrogen, and DDT was observed near the end of the channel for a 25 percent hydrogen mixture. With the obstacles in place and no venting, DDT was observed near the end of the channel for a 15 percent hydrogen mixture. With the obstacles in place and 50 percent venting, DDT was observed at the end of the channel for a 20 percent hydrogen mixture. No tests were done with 13 percent venting with obstacles, but tests done without obstacles indicate that in a 25 percent hydrogen mixture, DDT occurred closer to the ignition point with 13 percent venting as opposed to no venting. The main conclusions of the study was that 50 percent venting was successful in reducing flame acceleration, especially when no obstacles were present. However, for the 13 percent venting, the turbulence produced by the vents outweighed the mitigating effect of the vents, and as a result, flame acceleration was promoted for mixtures containing more than 18 percent hydrogen.

As in the SNL tests, in the present study, we are also interested in the effect of venting on flame acceleration and DDT in hydrogen-air-steam mixtures in vessels with repeated obstacles. The transverse dimension of the vessel used in the present investigation is much smaller than that of the SNL vessel, but the L/D is much larger (e.g., 78 for the present tests and 14 for the SNL tests). Although the scaling of DDT depends critically on the transverse dimension D, it is important that the vessel length be sufficiently long for the flame to accelerate to velocities on the order of the speed of sound of the product gases. For example, in the SNL tests, DDT typically occurred at the end of the vessel; the larger L/D of the present vessel allows more distance for flame acceleration and DDT. Also investigated is the influence of initial mixture temperature on flame acceleration and DDT with venting present.

3. EXPERIMENTAL DETAILS

The DDT experiments with venting were carried out in the BNL High-Temperature Combustion Facility (HTCF) which is a 27-cm-inner diameter, 21.3-m-long heated detonation vessel. The standard detonation vessel (see Figure 1.1) is made up of seven equal-length flanged sections. A detailed description of the HTCF detonation vessel, the gas handling system, and other auxiliary equipment can be found in Ciccarelli et al. (1996). The detonation vessel is located inside a 3-meter-diameter tunnel which is roughly 3 meters below grade. All combustible gases are stored on a ground-level gas pad located about 100 meters from the tunnel. The experiments are carried out remotely from a control room which is also located on ground level, and an interlock system is in place which requires all personnel to evacuate the tunnel before a test is performed.

For these experiments, the main modification to the detonation vessel was the addition of four vent sections which were inserted between pipe sections. A schematic of the venting configuration is shown in Figure 3.1, and a photograph of the apparatus equipped with the vent sections is given in Figure 3.2. These vent sections consist of two standard pipe-crosses butt welded together, as shown in the photograph in Figure 3.3. The vent opening is extended away from the vessel surface by a "vent chimney," which consists of a 0.4-meter-long section of pipe. Both the inner diameter of the pipe-cross and the vent chimneys are identical to the existing HTCF straight pipe sections. Therefore, the total vent area per vent section is four times the cross-sectional area of the straight pipe section. Since there are four vent sections, each with four vent openings, the ratio of vent opening area versus total vessel surface area is 4(D/L), where D and L are the vessel diameter and length, respectively. This yields a vent area ratio of 0.05, or a vent area of 5 percent of the total vessel surface area. The welded pipe-crosses are mated to the straight pipe section using compatible flanges. The length of a vent section is 1.52 meters which is exactly half the length of a standard HTCF straight section. In order to maintain the same total vessel length-to-diameter ratio (e.g., 78) as the vessel without the vent sections, two of the straight sections are not utilized in the present experiments. In this way, all the straight pipe sections are separated from each other by a vent section.

Custom-designed ceramic heater blankets and insulation jackets were used on the vent sections. The heater and insulation materials are the same as the ones used in the straight pipe sections (Ciccarelli et al., 1996). The vent chimneys were wrapped in insulation but were not actively heated.

As shown in Figure 3.4, aluminum vent covers are used to cap the vent openings during evacuation of the test vessel. The aluminum caps are 1-cm thick and 34.3-cm in diameter, resulting in a 1.6-cm overhang relative to the vent chimney outer diameter. A vacuum tight seal is obtained by a Viton o-ring which is located between the outer edge of the vent chimney and the vent cover. A 5-mm-wide o-ring groove is machined into the edge of the vent chimney. Clips, which are mounted on blocks welded to the vent chimney, grasp the outside edge of the vent covers. There are four clips per vent cover. These clips serve two purposes: (1) hold the bottom covers in place and (2) provide some clamping force on the covers in order to create a seal at the o-ring. Once the vessel is under vacuum, the clips on the top vent covers are removed, and the clips on the bottom covers are left on to avoid them falling off after the test gas is loaded to atmospheric pressure. During energetic tests, where high pressure develops inside the vessel, the vent covers are dislodged at very high velocities. As shown in Figure 3.4, the vent covers are anchored to the vent chimney using wire rope. A 6.4-mm wire rope is wrapped around the vent chimney just below the blocks. A 4.8-mm diameter wire rope is anchored on the larger wire rope and looped through two holes drilled into the vent cover. In later tests, two wire ropes were used to anchor the vent cover to the wire rope placed around the vent chimney. In most cases, the wire rope was successful, but in several tests where transition to detonation occurred,

the wire rope failed. For these very energetic tests, the vent covers typically bent upon impact with the floor or wall and had to be replaced with new covers.

The entire vessel was equipped with obstacles, similar to those used in the DDT tests performed without venting (Ciccarelli, 1996). The obstacles consist of 1.9-cm-thick orifice plates, with a 27.3-cm-outer and 20.6-cm-inner diameter, yielding a blockage ratio of 43 percent. The orifice plates are equally spaced at one tube diameter spacing (i.e., 27 cm). This spacing is maintained by fastening the orifice plates to threaded rods with nuts on either side of each plate. There are six equally spaced, circumferentially mounted, 1.9-cm-diameter threaded rods. The threaded rods are anchored to the vessel at vessel flange locations. That is, the threaded rods are fixed at one end of the vessel section to special orifice plates, that have outer diameters larger than the vessel inner diameter, thus allowing these plates to be sandwiched between each pair of vessel flanges. The other end of the threaded rods are allowed to slide freely in order to accommodate for thermal expansion during heating of the vessel.

A flame is ignited in the test vessel by a standard diesel engine glow plug centrally mounted on one of the vessel end plates. The glow plug is powered through a 120/12 VAC step-down transformer. Depending on the initial mixture temperature, ignition occurs between 10 and 20 seconds after the power is first applied to the glow plug.

The straight pipe sections are equipped with two sets of five instrument ports on opposite sides of the vessel. The first and last pair of instrument ports on each pipe section are 30.5 cm from the inside face of the end flanges, and the internal ports are 61 cm apart. There are no instrumentation ports on the vent sections. Photodiodes and thermocouples were used to measure time-of-arrival of the flame. For very slow moving flames, the light emitted from the reaction zone is insufficient to be detected by the photodiodes. Therefore, for most runs, four thermocouples were placed in the first half of the vessel in order to capture the initial phase of the flame acceleration process. In a limited number of tests where very weak mixtures were tested, the thermocouples were placed in the center of all the pipe sections in order to track the flame over a longer distance. Initially, photodiodes were placed just before and just after each vent section in order to obtain the average velocity across each of the straight pipe and vent sections. Later, a third photodiode was placed at the midpoint of each pipe section in order to better capture the flame acceleration process between vent sections.

Two piezoelectric pressure transducers (e.g., PCB113) were used to measure explosion front pressure. The sensitivity of the pressure transducers were 73.5 mV/atm (5 mV/psi), which is too low to measure any mild isochoric pressurization during benign flame acceleration. In most cases, a pressure transducer was located in the second-to-last instrumentation port before the last vent section and the second port just after the last vent section.

In a limited number of tests, the vent cover opening times were measured using microswitches mounted on the vent chimneys and depressed by the vent cover overhang. Each vent cover had a microswitch, but only one signal from each vent section was recorded in the control room. In each vent section, the four microswitches are electrically connected in series, such that a signal is recorded from the vent section once the first cover dislodged.

The signal from the photodiodes, pressure transducers, and vent cover switches were recorded on three digital LeCroy oscilloscopes. The thermocouple signals were recorded on a slower PC-based data

acquisition system as described in Ciccarelli et al. (1996). A video camera was also installed to monitor each test and to record the sequence of vent-opening events that occurred during each test.

3.1 Test Matrix

The tests were performed in hydrogen-air-steam mixtures at initial temperatures up to 650K. The test matrix for these venting tests excluded sensitive mixtures due to potential damage to nearby equipment in the tunnel. The concern is that a violent explosion may occur in the tunnel as a result of the venting of unreacted mixture ahead of the flame. Although there is no potential threat to personnel, there is the possibility of damage to unprotected equipment in the tunnel, including the vessel insulation. In order to minimize this threat, the test mixture was limited to those mixtures where a detonation could not be transmitted from inside the vessel into a cloud of combustible mixture outside the vent opening. The criteria used to establish this limiting mixture composition was the critical tube diameter criterion. The critical tube criteria states that in order for a detonation to transmit from a confined geometry, such as a tube, into an unconfined geometry, the tube diameter must be at least 13 times the mixture detonation cell size (Guirao et al., 1989). This is very conservative since it does not consider the weakening of the detonation in turning the corner into the vent chimney and the mixing of the test gas with the air outside of the vent.

Once the tests were started, it became apparent that the explosion front over pressure would dictate the probability of damage and not the mixture detonation cell size. This is important since the AICC and detonation pressures decrease with increasing initial mixture temperature, whereas the mixture sensitivity increases (i.e., cell size decreases) with initial temperature. For example, the AICC and detonation pressures for hydrogen-air mixtures at an initial temperature of 300K are about double that at 650K (Ciccarelli et al., 1996). For a given mixture at a fixed initial temperature, the detonation pressure is about double the AICC pressure (Ciccarelli et al., 1996). Thus, the pressure generated by a deflagration in the choking regime (i.e., AICC pressure) at an initial temperature of 300K will be similar to the pressure produced by a detonation in the same mixture at 650K. For equipment safety reasons, this limited the range of tests that could be performed at 300K and 400K.

The only damage to equipment incurred during energetic tests was the bending of the vent covers resulting from the failure of the wire rope tethers. In order to maximize the number of tests which could be performed in the overall time frame, tests were first performed at 650K starting with lean hydrogen mixtures and gradually increasing the hydrogen concentration. Tests at room temperature were scheduled during the latter stages of this experimental program.

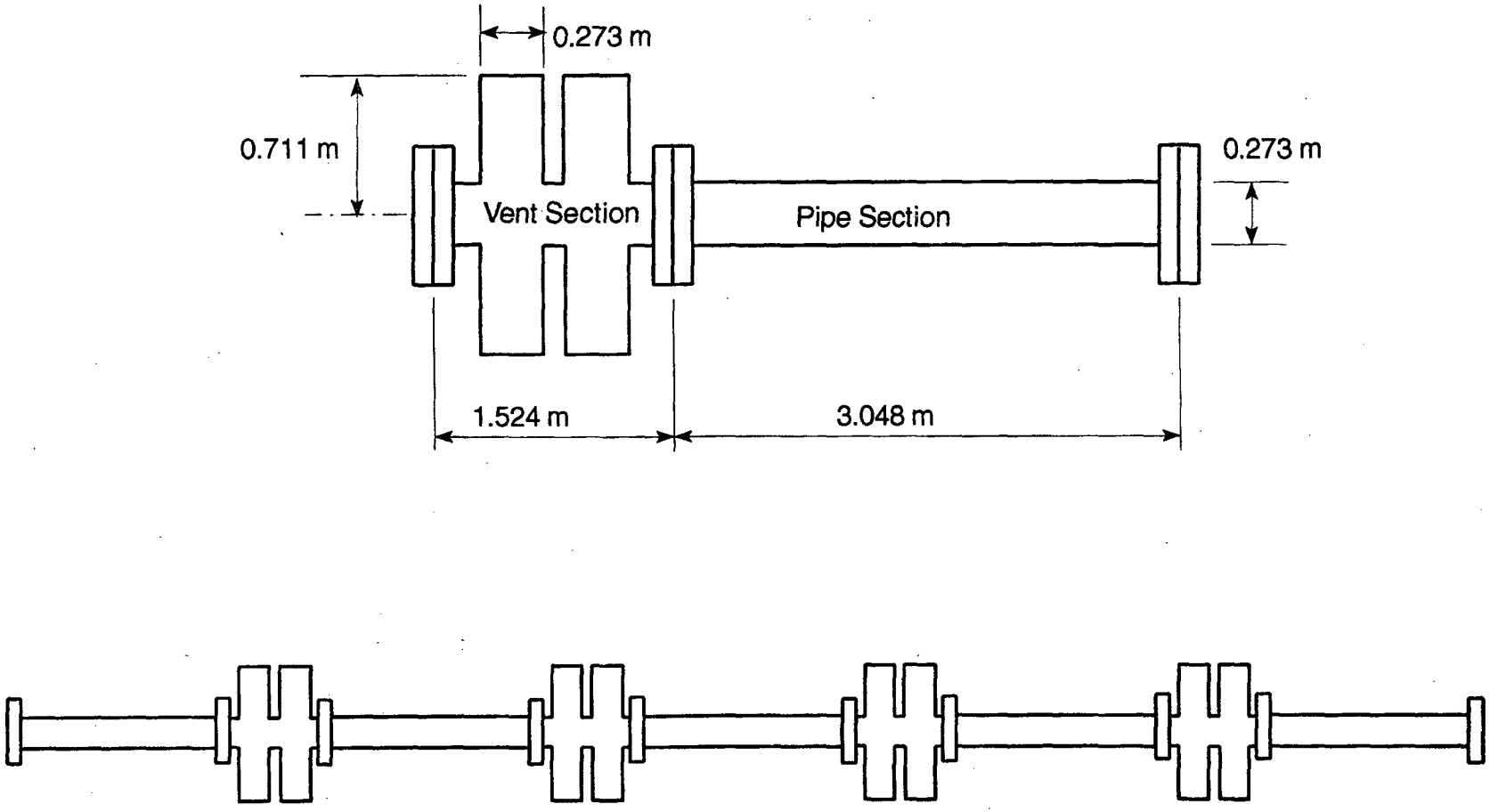

Figure 3.1 Schematic of the test vessel consisting of five tube and four vent sections

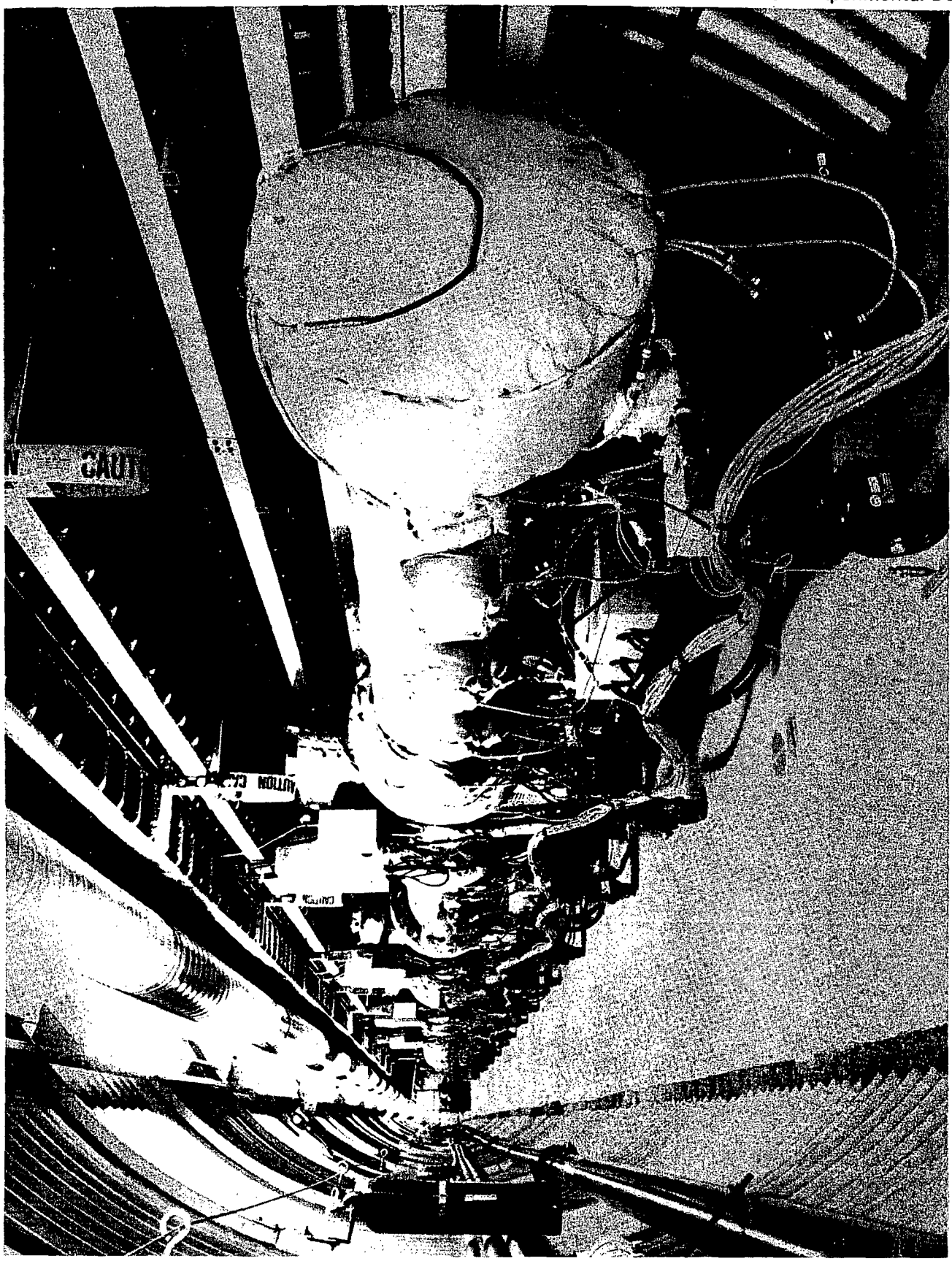

Figure 3.2 Photograph of the detonation tube equipped with vent sections

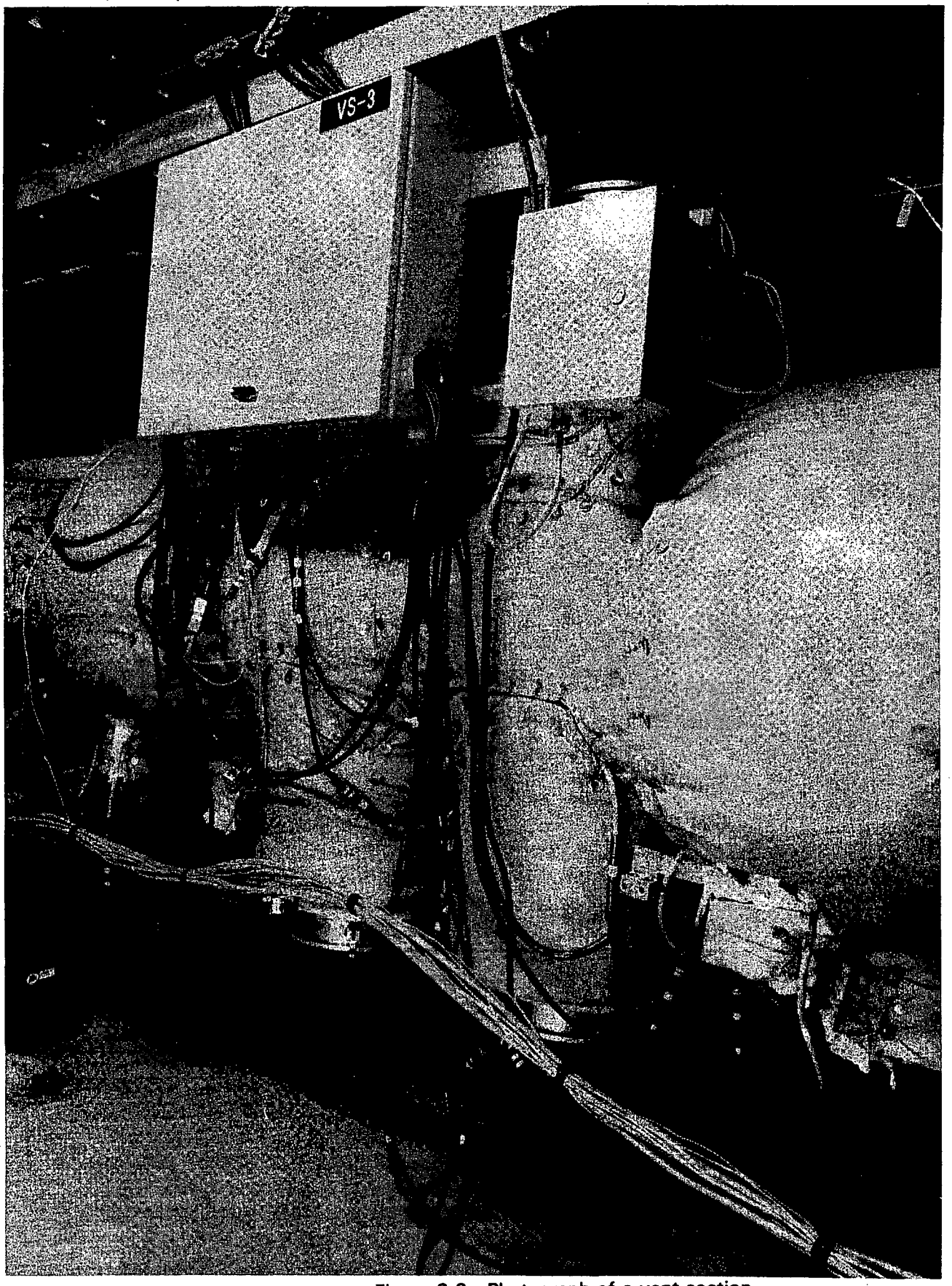

Figure 3.3 Photograph of a vent section

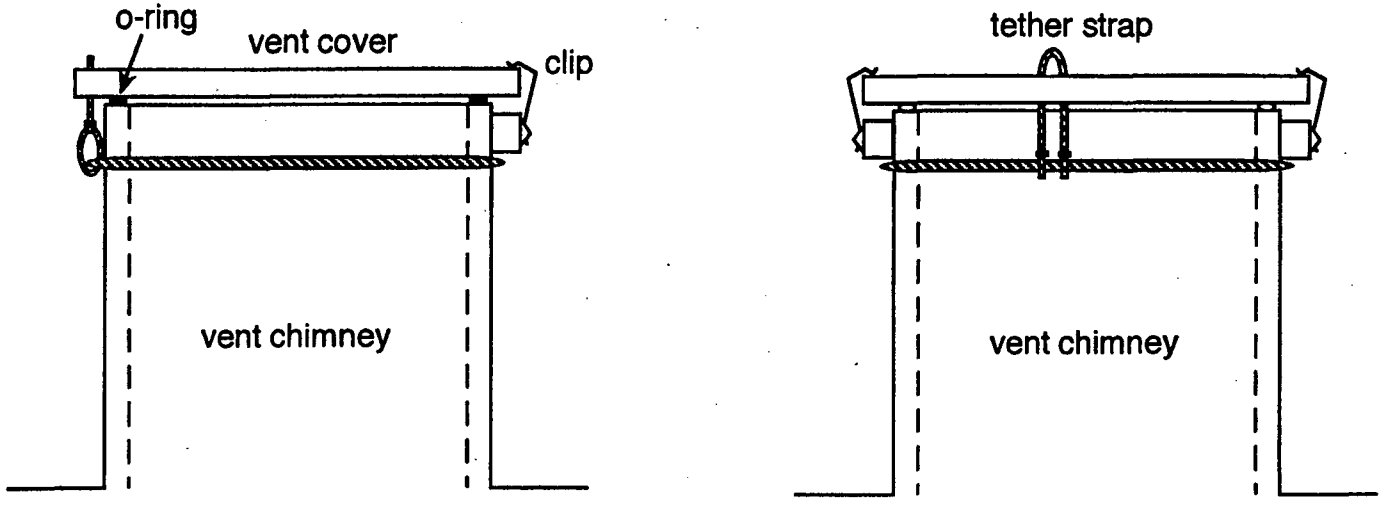

Figure 3.4 Schematic of vent cover tether strap and clip assembly

4. EXPERIMENTAL RESULTS

In this section, flame acceleration data will be presented for hydrogen-air-steam mixtures at various initial temperatures and an initial pressure of 0.1 MPa. The most sensitive mixture tested at each temperature was that mixture which first resulted in failure of the vent cover tethers. For lower temperature mixtures, due to the associated higher pressures, tether failures occurred even before DDT was observed. This was the case for the dry hydrogen-air mixtures at 300K and the hydrogen-air-steam mixtures at 400K and 500K. In the following sections, reference to experimental results from DDT tests *without* venting can be found in Ciccarelli et al. (1998). A summary of the experimental data from the present experiments is tabulated in Appendix A.

4.1 Flame Propagation at 300K

The flame velocity versus distance for four hydrogen-air mixtures at 300K is given in Figure 4.1. The arrows on the abscissa indicate the location of the center of each of the four vent sections. Note, the physical length of the vent section is 1.5 meters, but the active length of each vent section is only about 1 meter. The only mixture tested at 300K which resulted in any significant flame acceleration was the 12 percent hydrogen mixture. In the 9, 10, and 11 percent hydrogen mixtures, the flame reached a maximum average velocity of about 200 m/s by mid vessel and then decelerated to roughly the laminar burning velocity. For these benign burns, the light emitted from the flame is insufficient to obtain signals from the photodiodes. The measured velocities were obtained from time-of-arrival information from five thermocouples positioned at midspan of each tube section. This coarse spatial resolution precluded obtaining detailed velocity-distance profiles. The velocities indicated in Figure 4.1 are the average velocities measured over both a tube section and a vent section. Therefore, the actual velocity in the pipe sections are higher than the average, and in the vent sections, the velocities are lower than the velocities indicated in the figure. In order to obtain better resolution for the benign burns, a limited number of tests were performed with the thermocouples concentrated in the first half of the vessel. In most tests that resulted in a benign burn, only the vent covers in the first vent section (i.e., closest to the point of ignition) were found displaced from their original positions. During these benign tests, video camera visualization shows that while the first vent covers were dislodged from the vent chimney, for the remaining vent sections, the covers simply rocked like a lid on a pot of boiling water.

In the 12 percent hydrogen test in Figure 4.1, the flame quickly accelerates to a velocity consistent with flame propagation in the choking regime. The isobaric products sound speed for this mixture is 700 m/s. As shown in Figure 4.1, the average flame velocity across the first vent section is about 550 m/s, and the average speed in the second vessel section is roughly 800 m/s. Based on the available instrumentation for this test, it is impossible to know what the maximum velocity in the first vessel section was. In a test performed in the same vessel without the vents, the average flame velocity between 0.9 and 4.6 meters was 508 m/s, which is just slightly less than the 550 m/s velocity measured across the first vent. In the 12 percent mixture test without venting, the flame propagated in the choking regime at an average velocity of roughly 600 m/s with very little overshoot and velocity fluctuation. In the present venting test, the peak velocity in the 12 percent hydrogen mixture was 800 m/s. Therefore, it appears that the initial venting of the unburnt gas actually promotes flame acceleration. However, as the flame propagates further down the vessel, the average velocity drops to about 500 m/s. In the tests without venting, the leanest mixture where the flame propagated in the choking regime was 11 percent hydrogen, and in the tests with venting, see Figure 4.1, the choking limit is 12 percent. Therefore, there is only a very small influence of venting on the mitigation of flame

acceleration for hydrogen-air mixtures at 300K. We cannot comment on the effect of venting on DDT since no venting tests were performed at this low temperature .

4.2 Flame Propagation and DDT at 500K

Shown in Figure 4.2 is a plot of the flame velocity versus distance for hydrogen-air mixtures at 500K. At this temperature, all three propagation regimes were observed. In a 10 percent hydrogen-air mixture, the flame initially accelerated to a peak velocity of just over 200 m/s at the first vent section and then quickly decayed to the laminar burning velocity. For this particular test, the spatial resolution of the thermocouples was increased near the ignition point. From Figure 4.2, we see that the velocity actually increases across the first vent. As shown in Figure 4.3, in tests without venting, this mixture condition resulted in flame propagation in the choking regime. This provides another example that shows the general influence of venting is to mitigate flame acceleration. However, for this particular test, the initial flame acceleration up to and through the first vent is enhanced by the venting of the unburnt gases ahead of the flame.

In the 11, 12, and 13 percent hydrogen mixtures, the flame accelerates to an average velocity which is just under the speed of sound in the products for the mixture (see Figure 4.4). In these mixtures, a distinct cyclic pattern in the flame velocity distance profile develops in the last half of the vessel. The flame accelerates in the straight tube sections and decelerates across the vent. The vents appear to have a very local effect on the flame. There is only a very slight decrease in the overall average velocity as the flame propagates down the vessel. This is analogous to the drop in velocity after the initial overshoot observed in the tests without venting. It is not clear whether this cyclic pattern would continue indefinitely in a longer vented tube.

In the 15 percent hydrogen mixture, DDT occurs after the first vent section. The average velocity in the second vessel is just below the CJ detonation velocity for the mixture (e.g., 1525 m/s). The detonation velocity drops about 300 m/s across the second vent and then recovers in the third tube section to a velocity on the order of the CJ detonation velocity. At the third vent section, the detonation fails, and the velocity drops dramatically down to about 600 m/s. The flame then continues to propagate in the choking regime in the pattern described above. Figure 4.5 shows the measured flame velocity for the 15 percent hydrogen mixture along with the results obtained in the experiment without venting. Within the spatial resolution of the time-of-arrival measurements, in both cases, transition to detonation occurs at roughly the same location. Clearly, the main difference between the two is that the detonation eventually fails in the test with venting; however, before it fails, the average propagation velocity is similar to that observed in the no venting case.

Figure 4.4 shows the average propagation velocity measured over roughly the last half of the vessel for the hydrogen-air mixtures tested at 500K. The bars denote the range in the velocities measured over this distance. Also shown in Figure 4.4 are the theoretical CJ detonation velocities and the sound speed in the products assuming an isobaric combustion process. From this figure, one can see that the average velocities for the mixtures containing between 11 and 13 percent hydrogen are just below the speed of sound in the products which is consistent with propagation in the choking regime when no vents are present. The two data points shown for the 15 percent hydrogen mixture actually corresponds to the single test shown in Figure 4.2. In this experiment, after roughly 4 meters of travel, the flame velocity suddenly increases to a value of about 1400 m/s which is consistent with a DDT event. The flame then decelerates slightly after passing through the vent section and then recovers

to about 1400 m/s. At the third vent section, located at a distance of 12 meters, the flame velocity drops to 700 m/s, which is typical for the choking regime, and remains roughly at this velocity until the end of the tube. Therefore, in this one test, flame propagation in both the detonation and choking regime are observed. The two data points for 15 percent hydrogen in Figure 4.4 correspond to the average flame velocities when propagating within these two regimes. Without venting, the minimum hydrogen concentration at 500K for flame propagation in the choking regime was 8 percent hydrogen as opposed to the 11 percent hydrogen limit observed with venting. Without venting, the DDT limit was found to be 12 percent hydrogen, and with venting, DDT was observed at 14 percent hydrogen, albeit for only a short distance. Thus, for hydrogen-air mixtures at 500K, venting has a significant impact on both the choking and DDT limits. At 500K the tests with venting require more sensitive mixtures, than the no venting tests, for the flame to propagate in both the choking and DDT regimes.

4.3 Flame Propagation and DDT at 650K

The flame propagation results from the hydrogen-air mixtures at 650K are shown in Figure 4.6. In all the mixtures tested, with the exception of the 11 and 12 percent hydrogen mixtures which resulted in benign burns, flame acceleration is noticeably slower when compared to the results obtained at 300K and 500K. This is consistent with the observations made in the tests without venting. In Figure 4.6, there are two tests shown for 13 percent hydrogen. In one of the tests, the flame accelerates to an average velocity which is just below the speed of sound in the products. The acceleration-deceleration pattern which was observed so clearly in the 500K data takes some time to develop. In the other 13 percent hydrogen test, transition to detonation occurs after the third vent but fails shortly after the fourth vent. Transition to detonation is also observed in both the 14 and 15 percent hydrogen mixtures. As was the case in the tests without venting, the distance from the ignition point to the DDT location (i.e., detonation run-up distance) decreases with increasing hydrogen mole fraction.

Shown in Figure 4.7 is the average propagation velocity in the hydrogen-air tests performed at 650K along with the theoretical CJ detonation velocities and the speed of sound in the products. We see that the average propagation velocity in the 15 percent hydrogen mixture is consistent with a detonation wave. Also, the velocity excursions observed in the 13 and 14 percent hydrogen mixtures are consistent with transition to detonation. The only mixture tested that resulted in propagation through the entire vessel in the choking regime was 13 percent hydrogen. A repeat of this test resulted in DDT. Since 12 percent hydrogen resulted in a benign burn, we see that there is almost no choking regime for flame propagation in hydrogen-air mixtures at 650K, as was the case without venting. The DDT limit observed in the present experiments is 13 percent hydrogen, which is higher than the 12 percent hydrogen DDT limit observed in tests without venting.

The following table summarizes the observed choking and DDT limits for the hydrogen-air mixtures tested at all three initial temperatures, with and without venting.

Table 4.1 Choking and DDT limits for hydrogen-air mixtures

Temp (K)	Choking Limit		DDT Limit			
	No Venting	Venting	No Venting		Venting	
	% Hydrogen	% Hydrogen	% Hydrogen	d/λ	% Hydrogen	d/λ
300	11	12	15	1.0	NA	
500	8	11	12	1.5	15	5.5
650	11	13	11	5.5	13	11.9

A comparison of both the choking and DDT limits, with and without venting, indicates that venting plays a key role in mitigating both flame acceleration and transition to detonation.

4.4 Flame Propagation and DDT in Hydrogen-Air-Steam Mixtures

The propagation velocity versus distance plots for various hydrogen-air steam mixtures at 400K, 500K, and 650K are shown in Figures 4.8, 4.9, and 4.10, respectively. As shown in Figure 4.8, at 400K, the mixtures tested were limited to between 10 and 13 percent hydrogen in air with 10 percent steam dilution. In this range of mixture composition, only flame propagation in the slow deflagration and the choking regimes were observed. Note for the 10 and 11 percent hydrogen mixtures, velocity measurements were only obtained in the first seven meters of flame propagation from thermocouple data. However, based on the time that the vent covers opened, it is clear that the flame velocity decays to tens of meters per second by the end of the vessel. At 500K, the trends in the flame velocity versus distance data shown in Figure 4.9 are very similar to the results obtained in the tests performed at 500K without steam dilution, as shown in Figure 4.2. The sole exception is that DDT was not observed for the range of mixture composition tested--namely, up to 22 percent hydrogen. Shown in Figure 4.10 are the results for hydrogen-air mixtures diluted with 25 percent steam at 650K. Transition to detonation was observed in the 23 percent hydrogen mixture. For this test, the flame accelerated up to the first vent section and most likely transitioned in the pipe section just before the second vent. Note there is only one average velocity measurement taken between the first and second vent sections. This detonation then fails through the second vent section only to reaccelerate and transition to detonation for a second time in the pipe section between the second and third vent sections. The detonation then fails for a second time through the third vent section, and the emerging flame continues to the end of the vessel in a manner typical for flame propagation in the choking regime.

A summary of the observed choking and DDT limits for these steam-diluted, hydrogen-air mixtures is given in Table 4.2.

Table 4.2 Choking and DDT limits for hydrogen-air-steam mixtures

Temp (K)	Choking Limit			DDT Limit			
	% H2O	No Venting	Venting	No Venting		Venting	
		% H2	% H2	% H2	d/λ	% H2	d/λ
400	10	12	12	18	0.7	N/A	
500	25	14	15	24	1.5	N/A	
650	25	16	18	19	0.8	23	5.7

As was the case in the dry hydrogen-air mixtures, venting increases the choking and DDT limit in steam-diluted, hydrogen-air mixtures. The most dramatic effect was observed in the 25 percent steam-diluted, hydrogen-air mixtures at 650K, where the DDT limit increased from 19 percent hydrogen without venting to 23 percent hydrogen with venting.

4.5 Pressure-Time Measurements

In a limited number of tests, pressure-time histories of the explosion were recorded. Two piezoelectric pressure transducers were used to measure pressure roughly one meter before and after the last vent section. Pressure traces obtained at these locations during the passage of a flame in a 20 percent hydrogen in air mixture with 25 percent steam dilution at 650K are shown in Figure 4.11. These pressure traces are typical for flame propagation in the choking regime. The top pressure trace, Figure 4.11a, corresponds to the pressure transducer located before the last vent section. This pressure trace is characterized by three distinct jumps in pressure followed by erratic pressure fluctuations. At the location of this pressure transducer, the flame is in the last part of the flame acceleration phase in between vents. In this phase, the propagation velocity is very close to the speed of sound in the products which is supersonic relative to the unburnt gas. Therefore, the pressure jumps are due to various shock waves produced ahead of the accelerating flame. Except for the initial 0.3-atm pressure jump, this pressure profile looks very similar to the pressure traces obtained in the flame acceleration tests without venting. The 2.2-atm overpressure associated with the second peak in Figure 4.11a is similar in magnitude to the pressures recorded in the same mixture in the tests without venting. As was shown for the tests without venting, based on the measured pressures and shock time of arrivals, the third pressure rise is due to the reflected shock wave off of the orifice plate located 6.4 cm ahead of the pressure transducer. The initial pressure rise in the trace corresponds to a relatively weak Mach 1.1 shock wave. The pressure after the initial rise remains fairly constant except for the small spike at about 0.25 ms which probably corresponds to the reflected wave off the orifice plate ahead. Since the pressure remains constant behind the shock wave, this indicates that the shock wave does not decay in strength as it propagates.

The pressure trace in Figure 4.11b obtained from the pressure transducer after the last vent corresponds to a series of decaying shock waves (i.e., blast waves) as opposed to the constant strength shock waves observed in the pressure trace before the vent. The blast waves observed after the vent are due to shock wave diffraction in the vent section and rarefaction waves generated by the

venting of high pressure gas. In this pressure trace, the peak overpressure associated with the initial pressure pulse is 0.6 atm, which is double the initial overpressure measured in the pressure transducer before the vent (see Figure 4.11a). Based on the fact that the initial pressure pulse after the vent is decaying and has a larger peak pressure than the precursor shock before the vent, one can conclude that the initial blast wave measured after the vent does not correspond to the propagation of the precursor shock wave before the vent. Using these pressure traces and the flame time-of-arrival information from the photodiodes, a detailed description of the flame propagation in the choking regime will be presented later in the report.

4.6 Vent Cover Release Times

As described in Section 3, each of the vent covers maintains a switch closed when it is securely attached to the vent chimney. When the vent cover is blown off the vent chimney as a result of vessel pressurization, the switch opens. The switch is part of a simple electrical circuit which generates a voltage spike when the switch is opened, thereby providing an opening time for the vent cover. This distance which the cover must travel for the switch to open varies from switch to switch, but on the average, it is about 5 mm. All four vent cover switches from each vent section are electrically wired in series so that only one signal is obtained per vent section. Therefore, the signal from each vent section is generated at the time the first of the set of four vent covers is lifted. Due to the passive method of ignition, i.e., glow plug, a zero time corresponding to ignition is not available. The oscilloscopes were triggered using the switch signal from the first vent section. The signal from the vent covers and the photodiodes were recorded on the oscilloscopes so that a comparison between the opening times of the vent covers and the time of arrival of the flame at the respective vent sections could be made. In the case of slow deflagrations, where the flame time of arrival was measured using thermocouples, no direct comparison can be made since the thermocouple signals were recorded on a separate data acquisition system.

Shown in Figure 4.12 is a distance-time plot for three different tests which resulted in flame propagation in the choking regime. The open symbols represent the time of arrival of the flame at the various photodiodes, and the closed symbols correspond to the vent opening times. Note, on this graph, time zero is taken as the time when the first vent cover opens. It is clear from this graph that all the vent covers open even before the flame reaches the first vent, and, therefore, the vent opening is not a local flame phenomenon. That is, the vents do not open as a result of local high pressure ahead of the flame. The vent opening times are consistent with a pressure pulse propagating the length of the vessel at roughly the speed of sound in the unburnt mixture. It is important to note that just a slight overpressure is required to sufficiently move the vent cover to open the switch. However, due to the low sensitivity of the pressure transducers used in the present study, there is no direct evidence of such a pressure pulse.

The results from Figure 4.12 are reproduced in Figure 4.13 along with the vent opening times from two tests where the flame propagates in the benign slow deflagration regime, demarcated by closed symbols. In these two tests, the flame accelerates to a maximum velocity of about 150 m/s by the first vent and then decelerates to a velocity approaching the laminar burning velocity. It is interesting to note that the vent opening times are similar for flame propagation in the choking and the slow deflagration regime even though the maximum flame velocities are very different. This is further evidence that the vent cover opening corresponds to the propagation of an acoustic wave down the length of the vessel far ahead of the flame.

The distance-time plot obtained for three tests which resulted in transition to detonation are shown in Figure 4.14. The flame trajectories, shown as open symbols, for each test are vertically staggered as a result of the different detonation run-up distances. Once the detonation is formed, the trajectories are fairly parallel. Indicated in this plot, with diamond symbols, is a test which resulted in the onset of a detonation wave before the first vent section. The composition of the mixture during this test is not fully known. The measured dry hydrogen concentration was about 27 percent; however, the amount of steam dilution is unknown. This experiment was not reported in any of the results presented earlier due to the uncertainty in the composition. This is the only test which resulted in the propagation of a detonation through the entire vessel. As can be seen from the Figure 4.14, the vent covers open shortly after the detonation passes the vent location. This lag in the opening time is largely due to the finite transit time for the shock wave to travel in the vent chimney. In the 14 percent hydrogen mixture at 650K, the first and second vent covers open before the flame arrives at each vent, respectively. This is similar to the behavior observed in Figure 4.12 for flames propagating in the choking regime. After transition to detonation is initiated, the vent covers open after the detonation passes the vent. Therefore, the start of the venting process is governed by local propagation phenomenon. For these cases, the detonation wave overtakes the initial pressure pulse which is responsible for opening the vent covers in the test where the flame propagates in the choking regime.

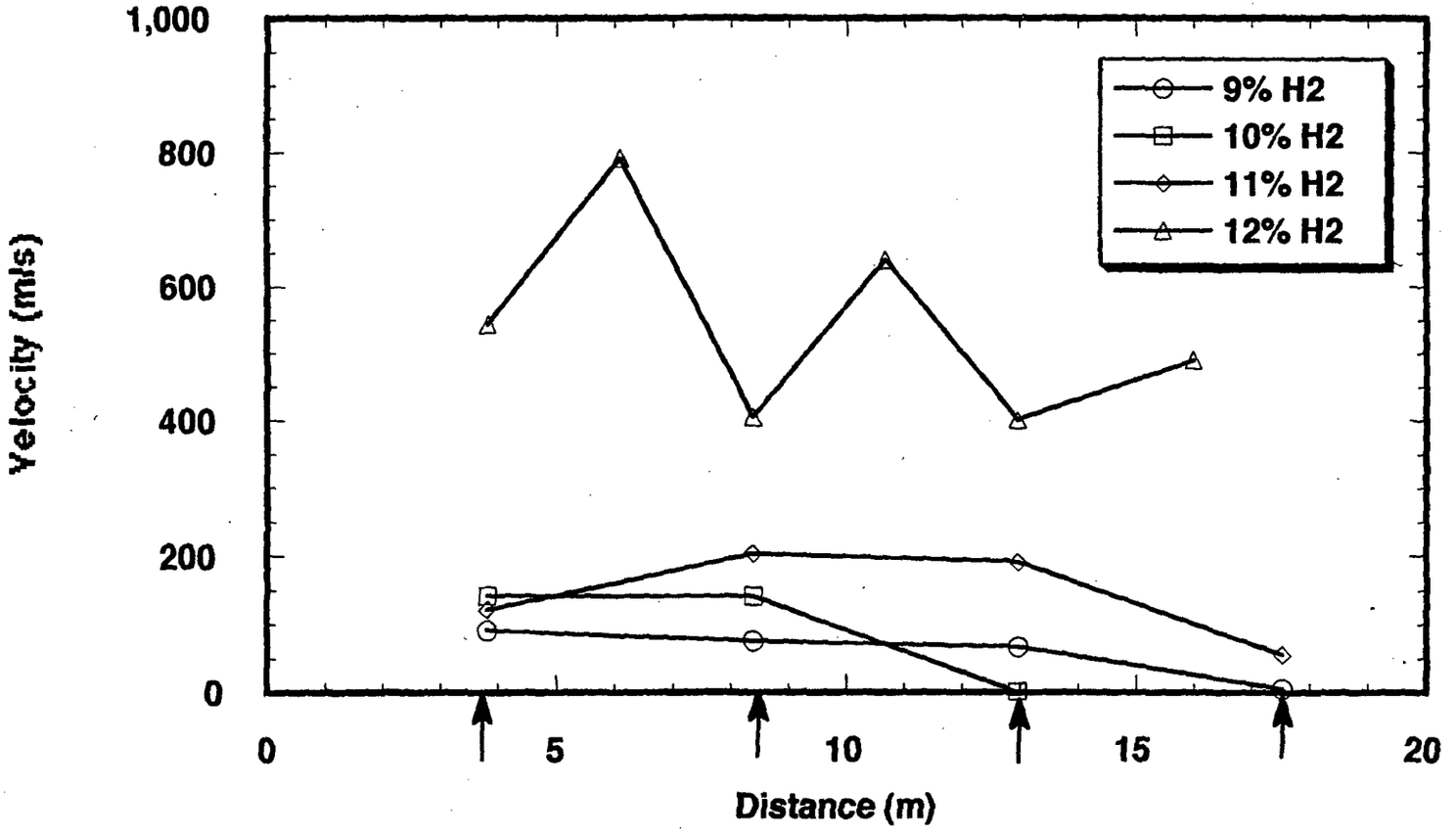

Figure 4.1 Combustion front velocity vs. propagation distance for various hydrogen-air mixtures at 300K

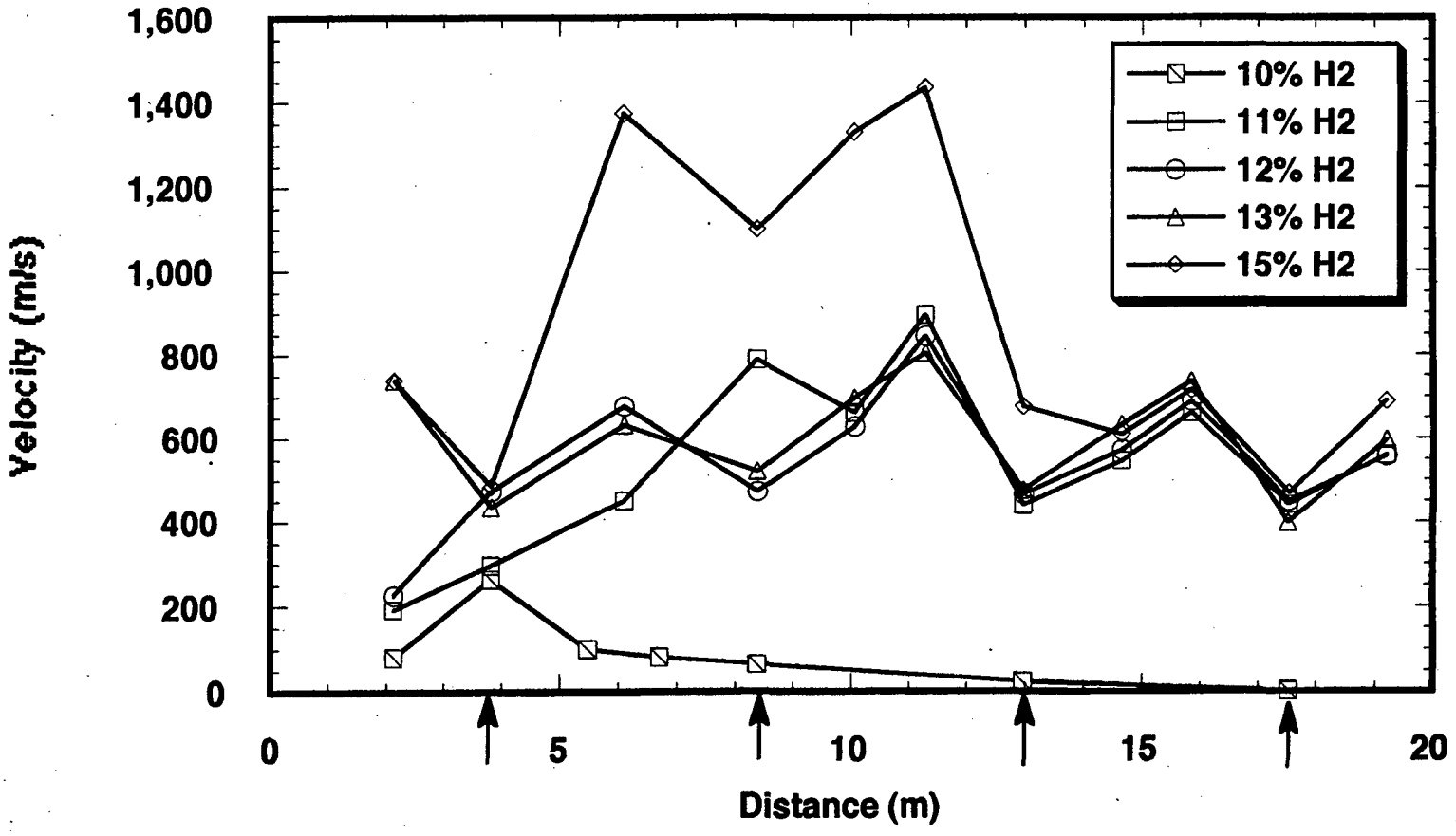

Figure 4.2 Combustion front velocity vs. propagation distance for various hydrogen-air mixtures at 500K

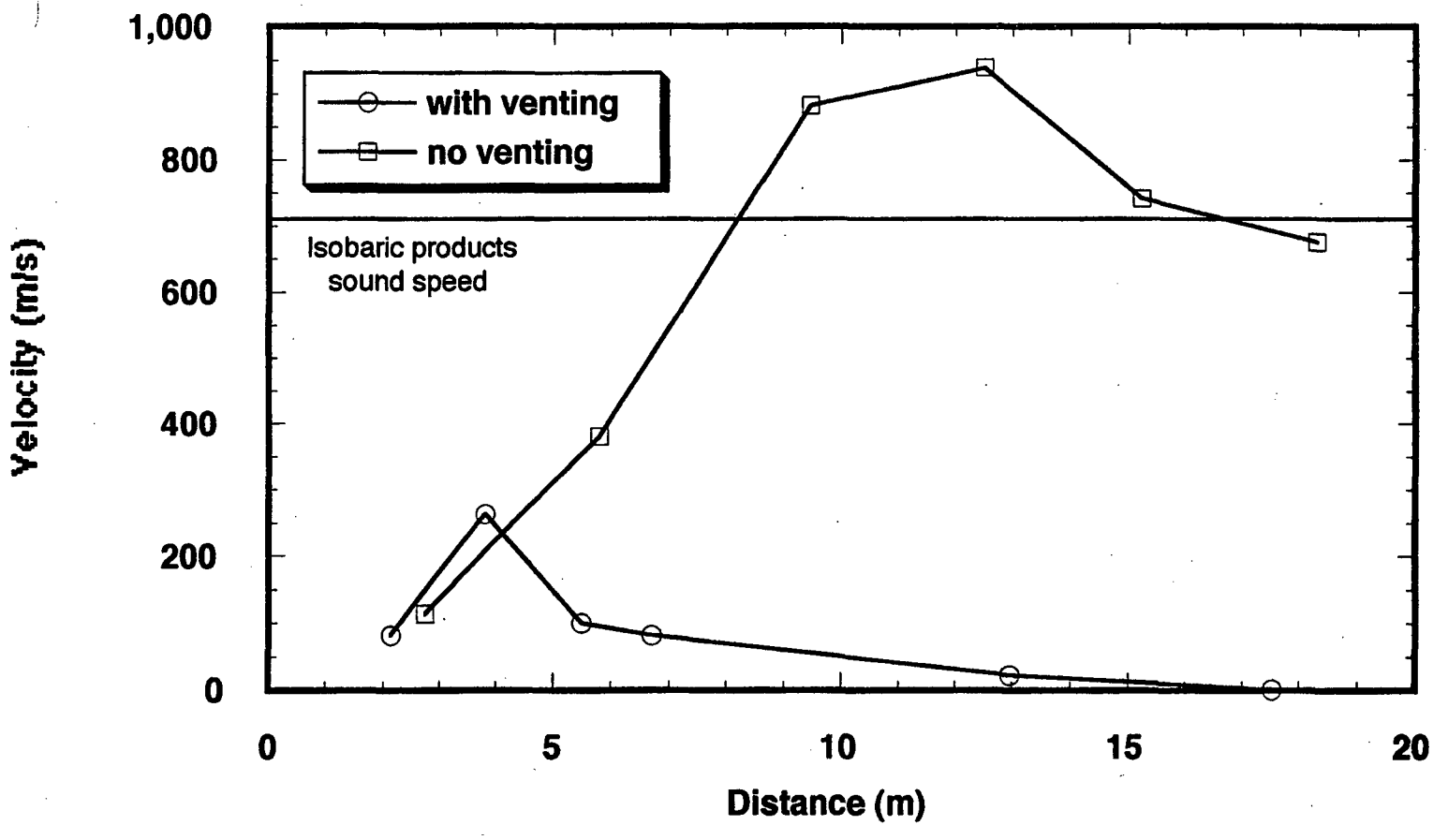

Figure 4.3 Comparison of the combustion front velocity vs. distance for a 10 percent hydrogen-air mixture at 500K with and without venting

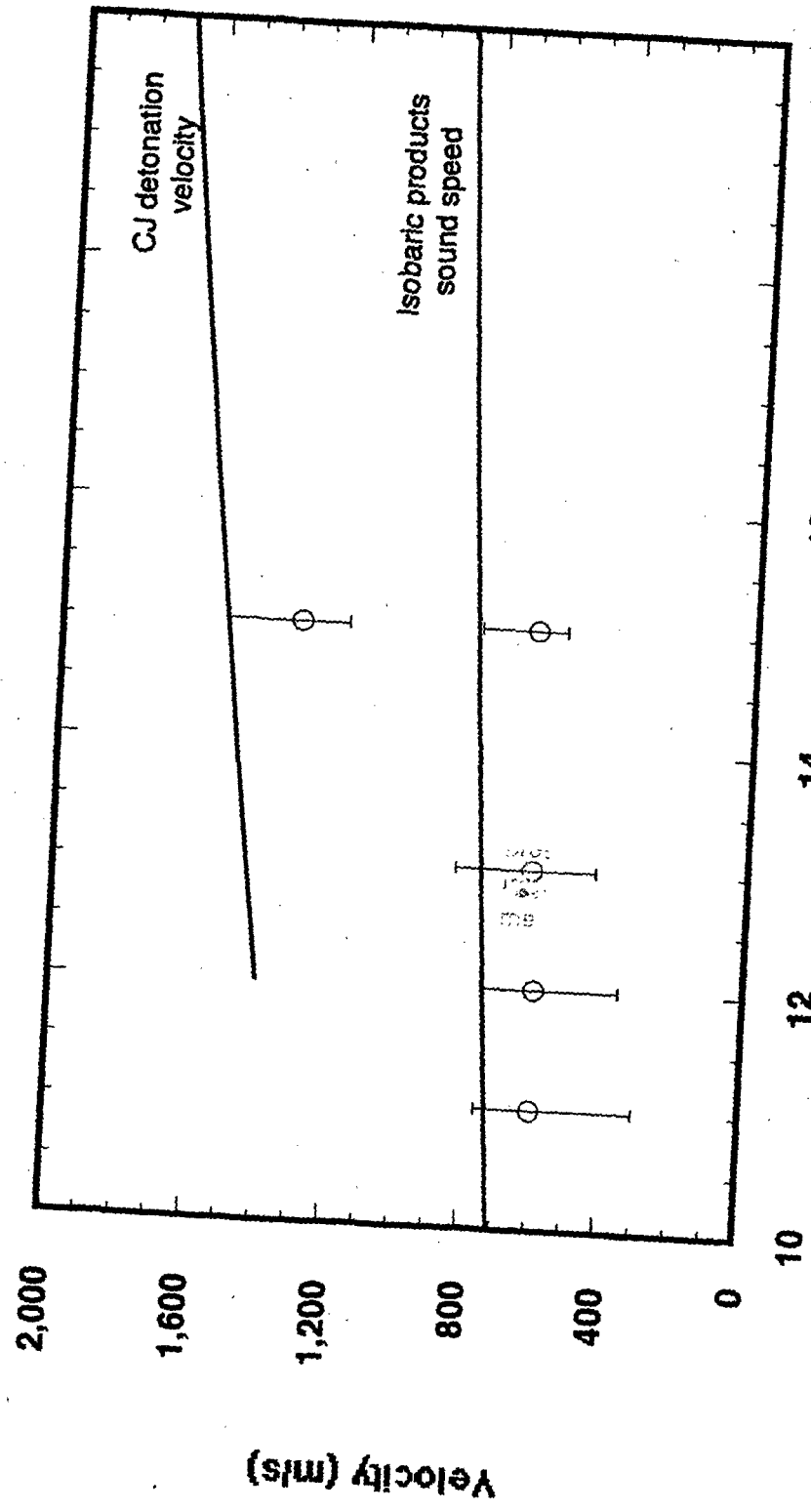

Figure 4.4 Average propagation velocity for hydrogen-air mixtures at 500K

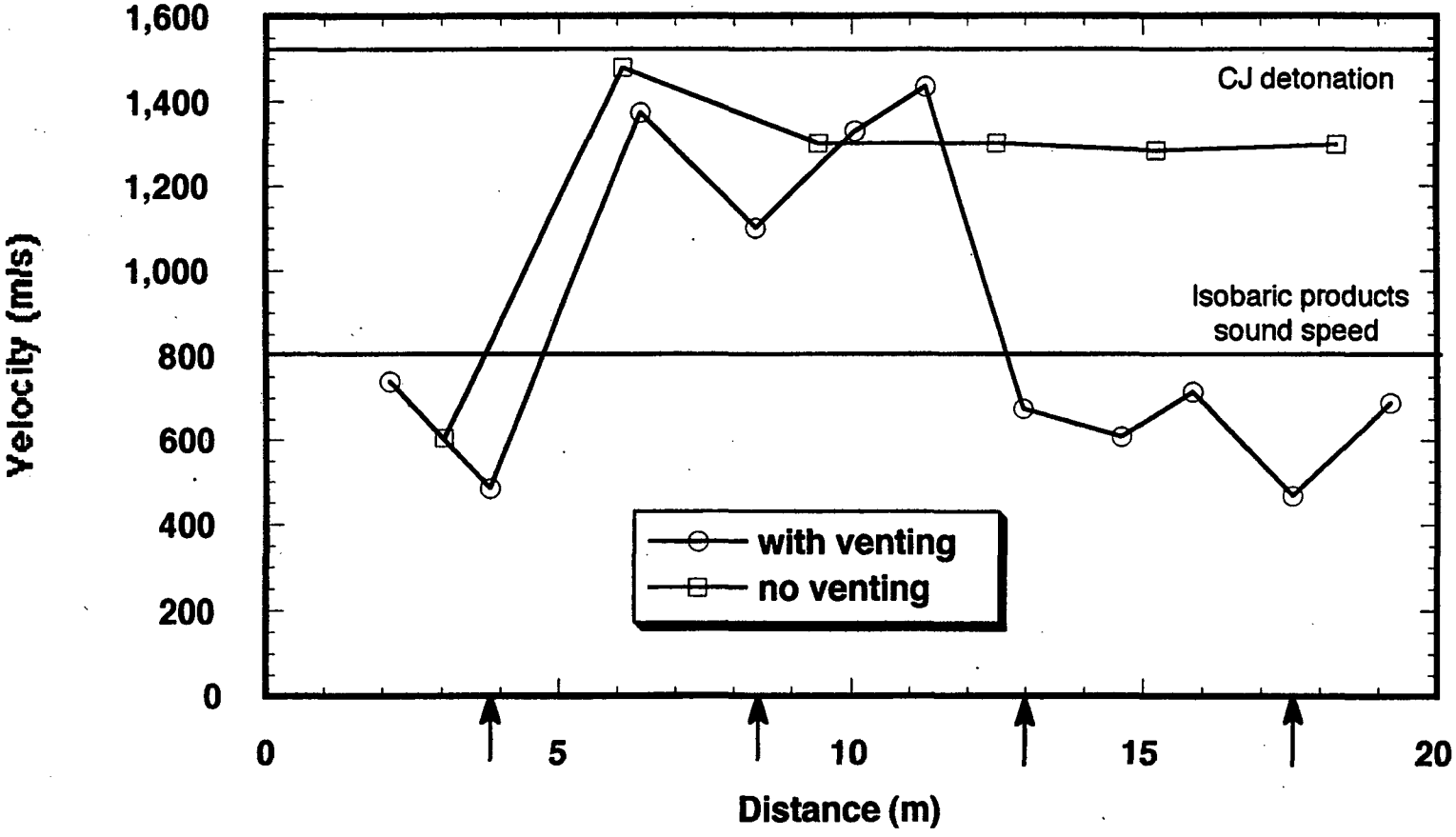

Figure 4.5 Comparison of the combustion front velocity vs. distance for a 15 percent hydrogen-air mixture at 500K with and without venting

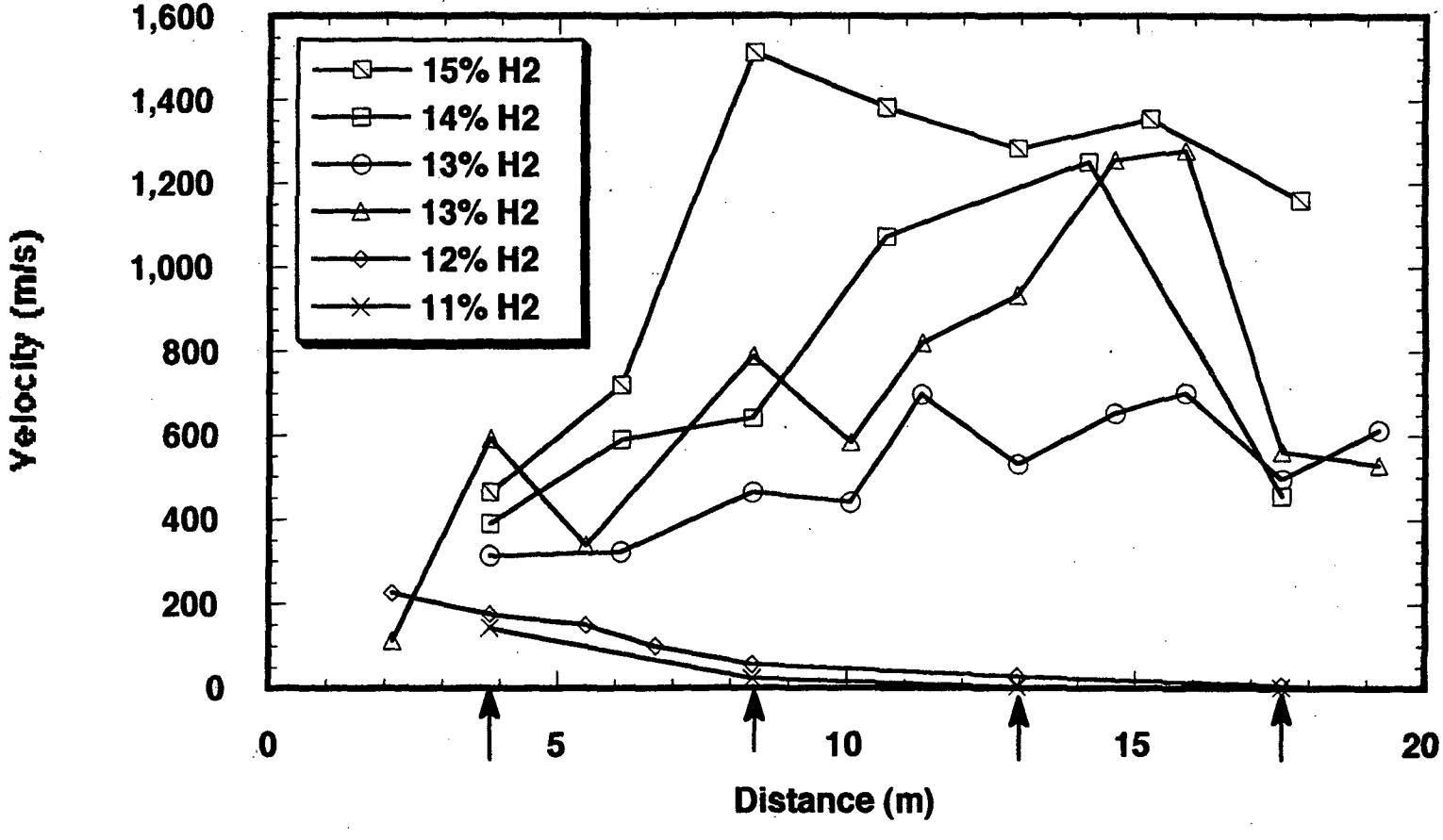

Figure 4.6 Combustion front velocity vs. propagation distance for various hydrogen-air mixtures at 650K

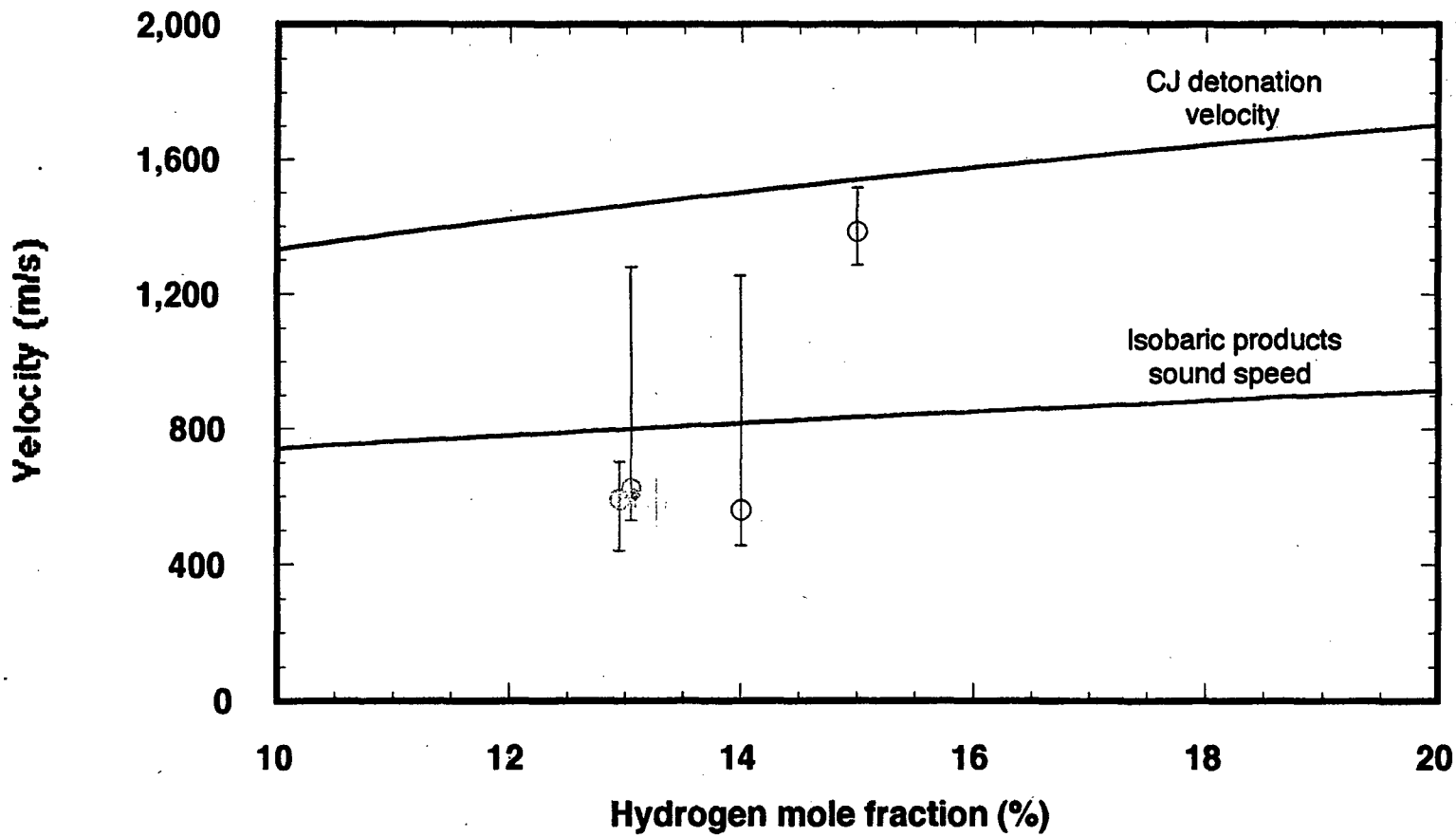

Figure 4.7 Average propagation velocity for hydrogen-air mixtures at 650K

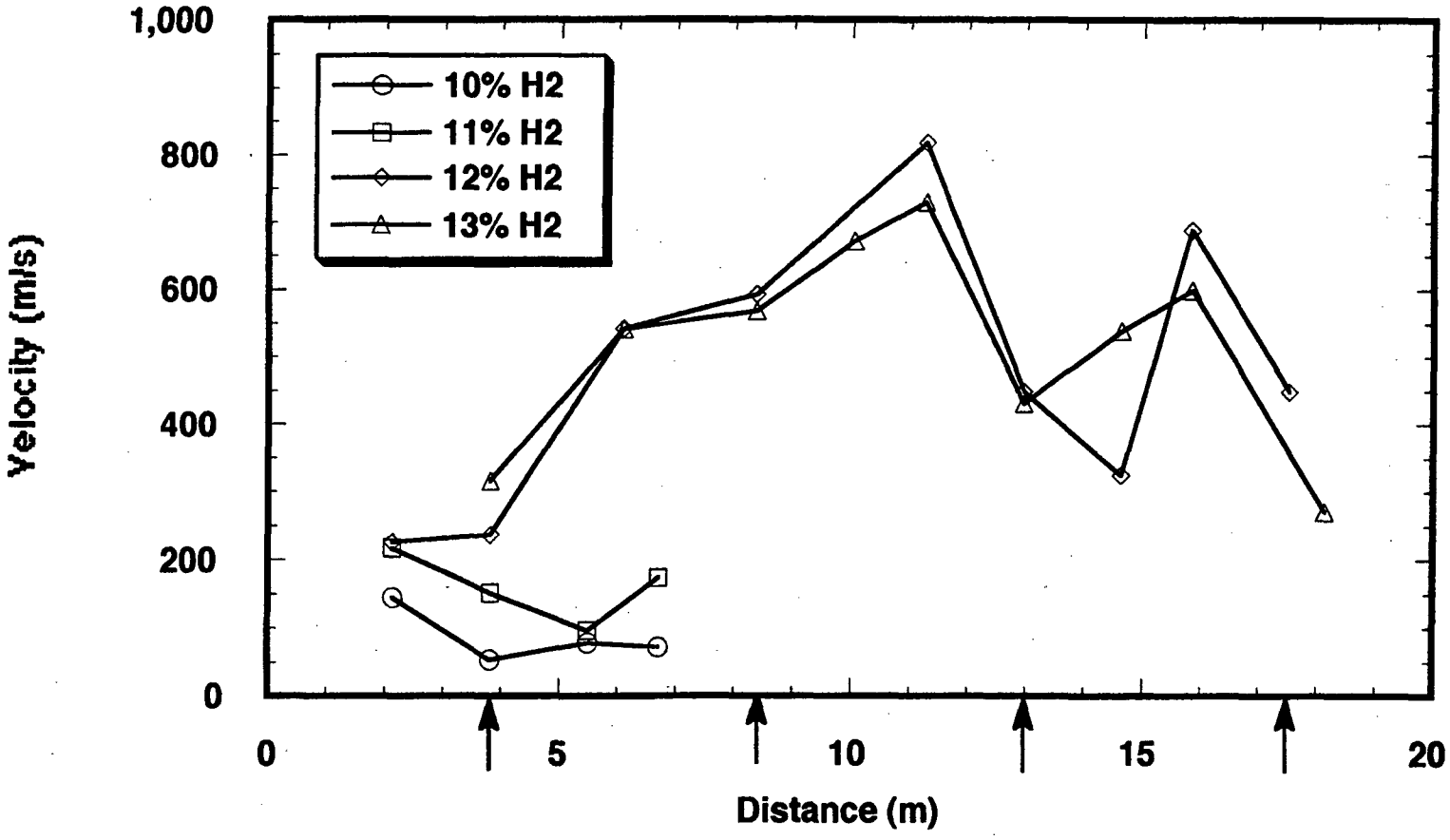

Figure 4.8 Combustion front velocity versus propagation distance for hydrogen-air-steam mixtures at 400K

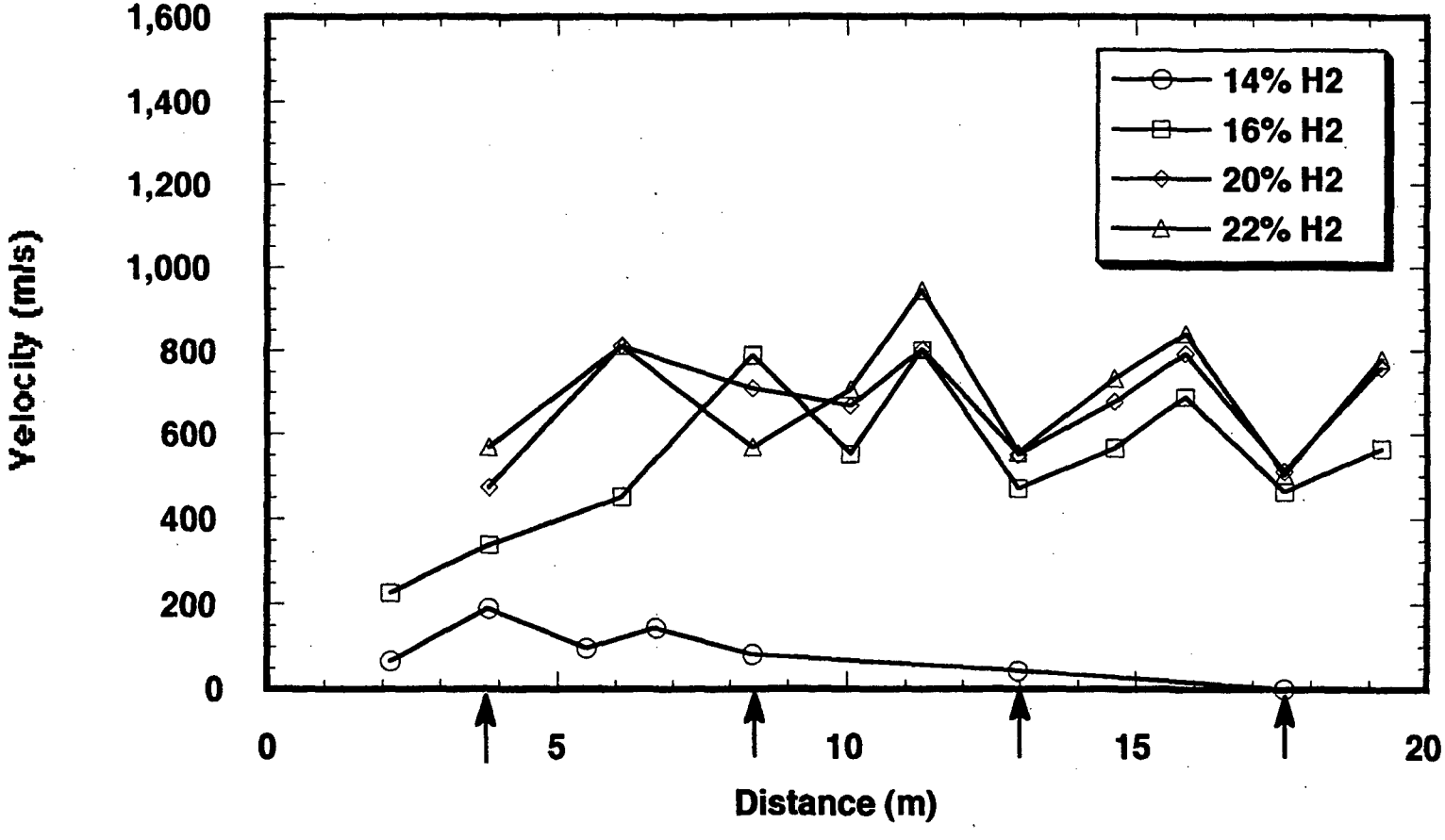

Figure 4.9 Combustion front velocity versus propagation distance for hydrogen-air-steam mixtures at 500K

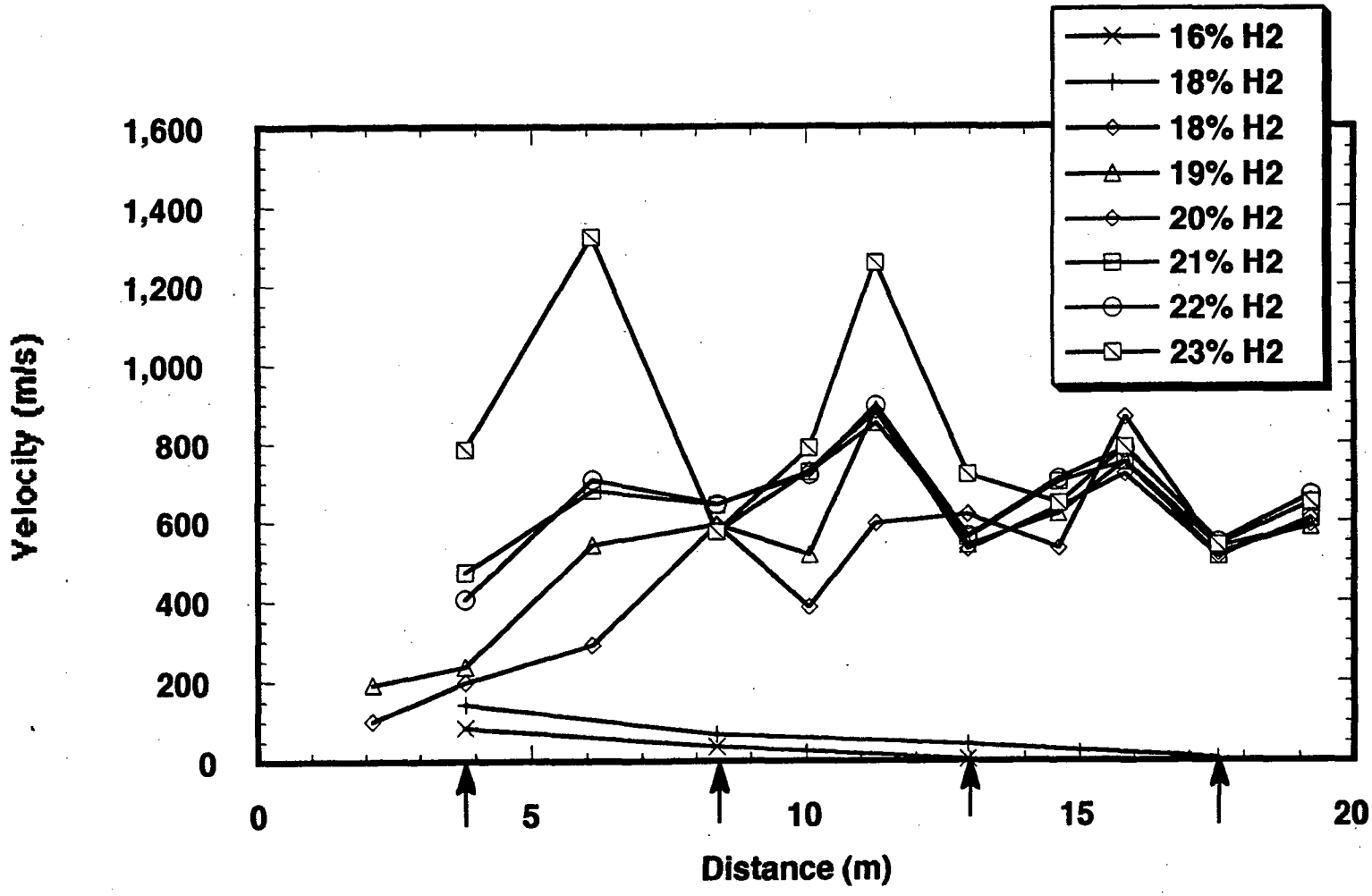

Figure 4.10 Combustion front velocity versus propagation distance for hydrogen-air-steam mixtures at 650K

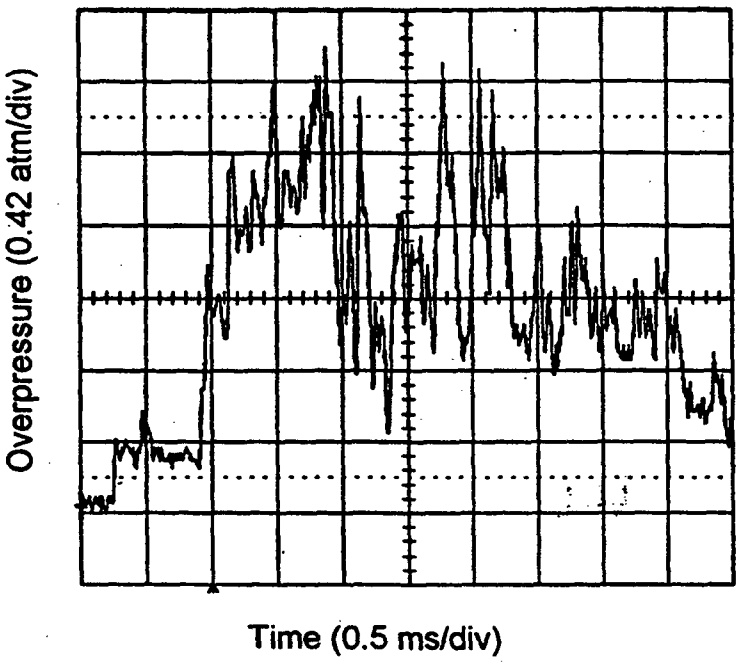

(a)

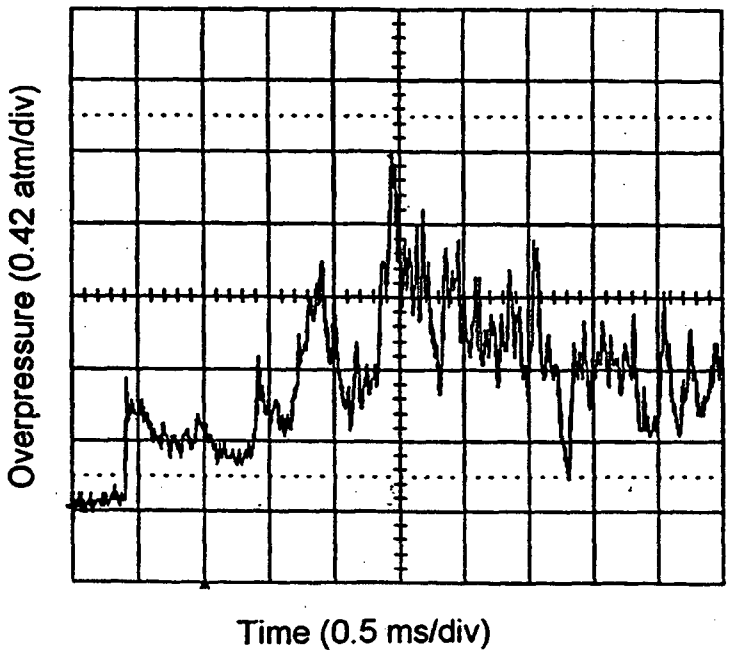

(b)

Figure 4:11 Pressure traces obtained before (a) and after (b) the last vent section for a 20 percent hydrogen in air mixture with 25 percent steam dilution at 650K

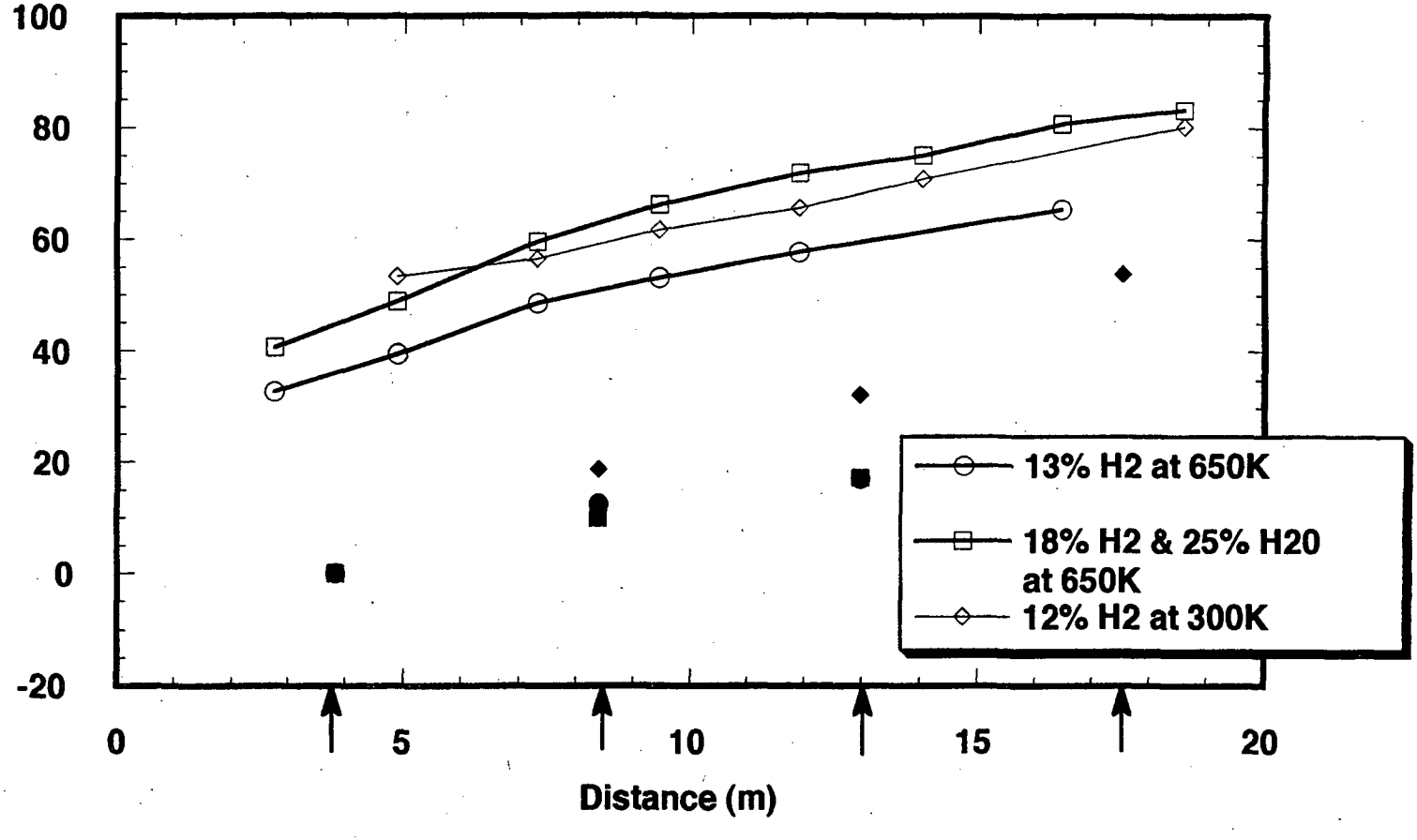

Figure 4.12 Flame time-of-arrival and vent opening times versus distance for various hydrogen-air-steam mixtures which resulted in flame propagation in the choking regime

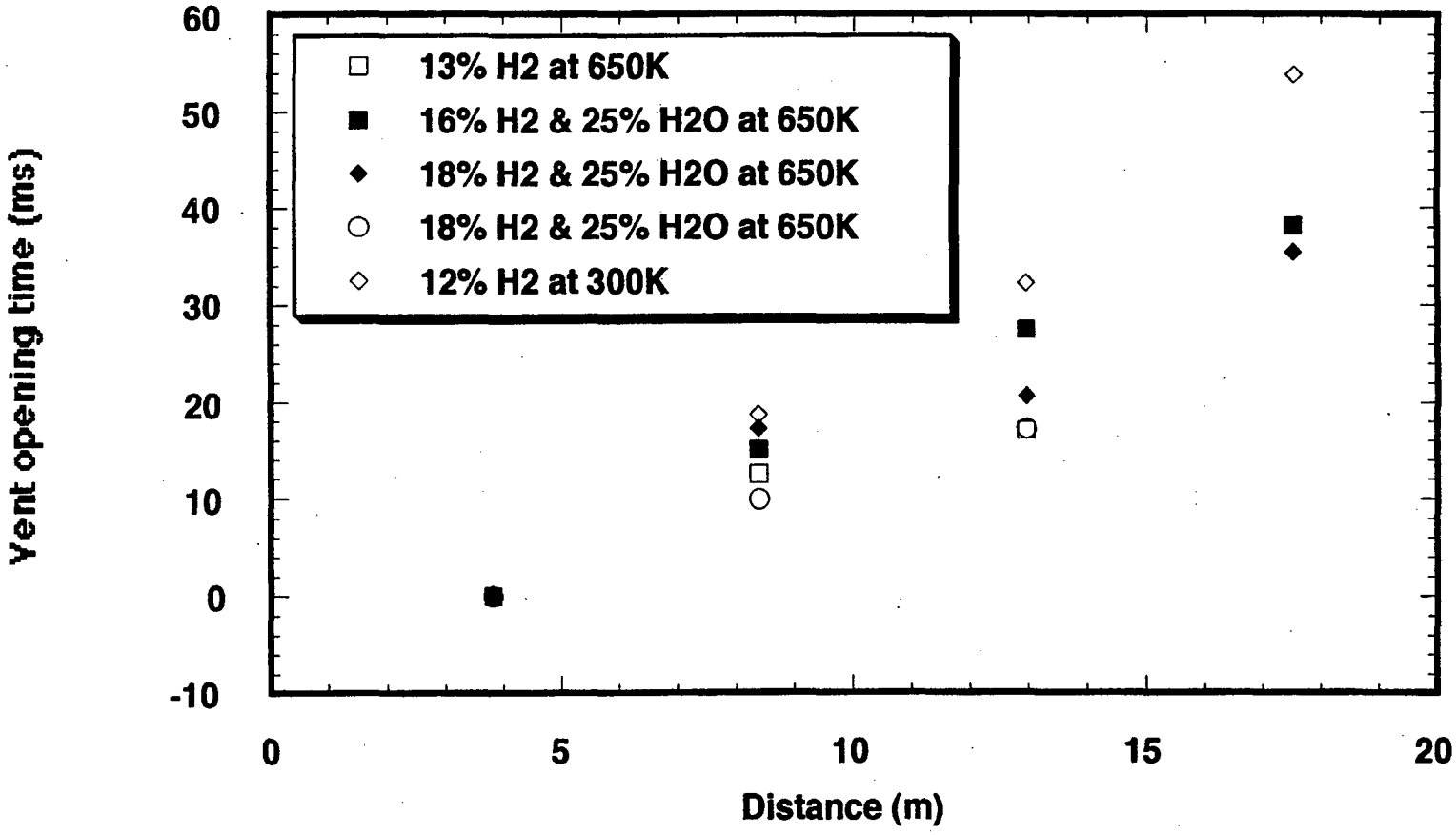

Figure 4.13 Vent opening times versus distance for various hydrogen-air-steam mixtures which resulted in flame propagation in the slow deflagration and the choking regime

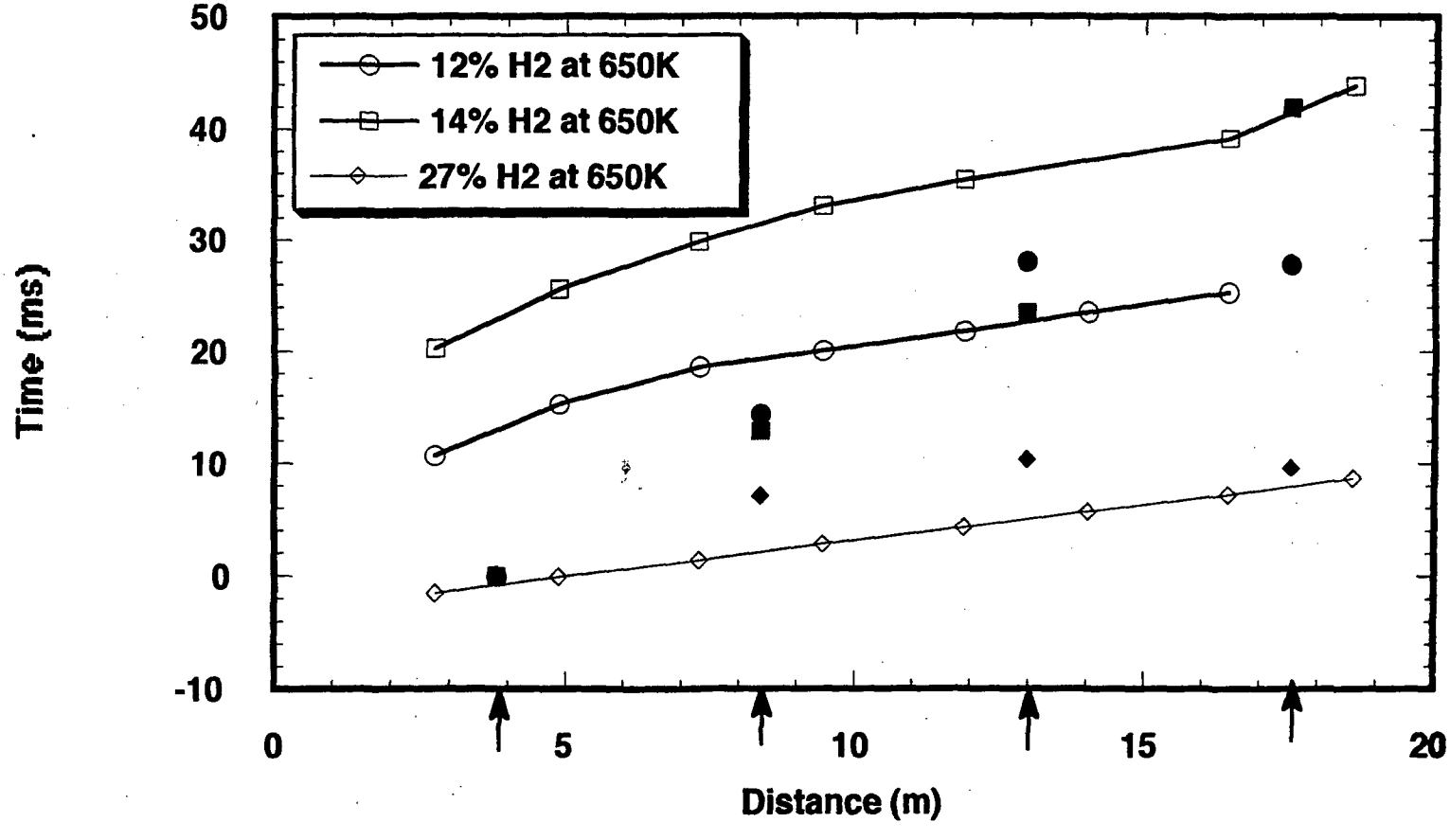

Figure 4.14 Flame time-of-arrival and vent opening times versus distance for various hydrogen-air-steam mixtures which resulted in flame propagation in the quasi-detonation regime

5. DISCUSSION

The experimental results have shown that flame propagation in the venting configuration used for this study can be classified into three regimes: (1) slow deflagration, (2) choking, and (3) detonation. These are the same classifications used to describe steady-state flame propagation in an obstacle-laden tube without venting (Ciccarelli, 1996). In the following sections, flame propagation in each of these regimes will be discussed in light of the experimental data. In the last section, recommendations on how the experimental data can be used for practical applications in the study of severe accidents in nuclear power plants is provided.

5.1 Flame Propagation in the Slow Deflagration Regime

In this section, a simple model is presented to investigate the influence of gas venting on flame acceleration in the slow deflagration regime. Since the flame velocities in the slow deflagration regime are relatively low, the vessel pressure can be assumed to be uniform, and a simple venting model can be used to describe flame acceleration. Chan et al. (1983) developed such a model to describe flame acceleration in an obstacle-laden rectangular channel with a perforated top plate. The obstacles consisted of thin plates extending from the vessel bottom plate to roughly half the channel height. Schlieren movies taken of the experiment show that the flow generated ahead of the flame resulted in pockets of recirculating gas in between the obstacles. These standing eddies between the obstacles are separated from the main flow above the obstacles by a shear layer. Early in the flame acceleration process, the flame is observed to follow the unburnt gas flow field as it is entrained in the standing eddy generated downstream of the obstacles. The increased flame surface area generated by the folding of the flame around the obstacle leads to larger volumetric burning rate and thus a larger displacement flow ahead of the flame, which results in flame acceleration. The burnout of these pockets was modeled simply by a flame moving transversely to the main flow into the pockets.

The following is a brief description of a modified version of the Chan et al. (1983) model, described above, with some typical predictions. A detailed description of the present model is given in Appendix B. Like Chan et al. (1983), the flow field is divided into the mainstream flow which exists in the core of the tube and the flow in the individual recirculation zones. A schematic showing the assumed flame structure in the nonvented pipe sections in the present study is given in Figure 5.1. Since the orifice plate spacing in the present experiment is roughly 9 times the plate height, it is assumed that the flow re-attaches to the vessel wall before the next obstacle setting up a recirculation zone just downstream of each of the obstacles. The recirculation zone which would normally exists upstream of the orifice plate is not shown in the figure and is not considered in the model.

The flow through any given orifice plate ahead of the flame is transient since the flame velocity increases with time and the flame position relative to the orifice plate changes with time. Therefore, the dimensions of the recirculation zone at each orifice plate will change with time. When the flame reaches an orifice plate, the outside edge of the flame in contact with the inner edge of the orifice plate is subjected to a high degree of strain. The stretching of the flame prevents it from burning directly into the recirculation zone. If the magnitude of the mainstream flow velocity is very high, one would expect that a flame could not cross the intense shear layer separating the mainflow and the recirculation zone (Chan et al., 1989). Instead, the entrainment of hot combustion products from the mainstream flow probably initiates combustion in the recirculation zone.

5. Discussion

As described above, the combustion process which occurs inside the recirculation zone is much more involved than the intended scope of this model. Therefore, a simple burning model is assumed where the volume of the recirculating zone is taken to be constant over time, and a characteristic constant burning rate is assumed. The volume of the recirculation zone, considered a parameter in the model, is governed by the distance downstream of the obstacle where reattachment occurs. It is assumed that the burning rate in the recirculation zone takes on a value based on the instantaneous burning rate of the main flame at the time the main flame reaches the obstacle. Note, in the model, the flame is assumed to be planar in the mainstream. The turbulent burning rates of the main flame and in the recirculation zone are given by two simple algebraic expressions which each include an empirical constant which must be specified. As the flame propagates in the vessel, vents located behind the flame eject burnt products and those ahead of the flame eject unburnt mixture. In the experiments, the bottom vent covers were held in place by clips. As a result, venting only starts after a critical pressure is reached and the clips disengage. In the model, the critical pressure is a parameter which is specified by the user.

The model prediction for flame velocity and vessel pressure versus flame propagation distance in an unvented vessel for a 10 and 11 percent hydrogen in air mixture at 300K is given in Figure 5.2. For these calculations, the recirculation zone length is taken to be five times the orifice plate width, and the burning rate proportionality constants in the recirculation zone and for the main flame are taken to be 0.05 and 0.66, respectively (see Appendix B for details). These constants were chosen so that the numerical predictions would be consistent with the experimentally observed choking limit. The staircase increases in the flame velocity observed in Figure 5.2 is due to the initiation of burning in the consecutive recirculation zones after each orifice plate. The numerical results indicate that flame acceleration is enhaced by increasing the hydrogen mole fraction. This is because both the laminar burning velocity and the density ratio across the flame increases with hydrogen mole fraction. In the case of 11 percent hydrogen, the flame velocity reaches a maximum of about 700 m/s, which is well above the 364 m/s speed of sound in the mixture. Since compressibility effects are not considered in this model, i.e., the density in the gas is assumed to be uniform, the solution beyond about 200 m/s is outside of the model assumptions. In both cases, the flame accelerates to a maximum and then decelerates as a result of the burning-out of the recirculation zones. In the 11 percent hydrogen case, after about 17 meters of travel, many of the recirculation zones burnout in a very short time and the flame velocity rapidly decays. Experimental observations indicate that once the flame achieves a velocity above the speed of sound in the unburnt gas, the flame continues to accelerate and then stabilizes at a velocity on the order of the speed of sound in the products or transitions to detonation and stabilizes at the CJ detonation velocity. Clearly, the deceleration predicted in the 11 percent hydrogen mixture in Figure 5.2 is nonphysical. However, flame deceleration similar to that observed in the 10 percent hydrogen mixture has been observed in mixtures near the lean flammability limit propagating in the slow deflagration regime.

The model prediction of flame velocity and vessel pressure for 10 percent hydrogen in air at 300K are given in Figure 5.3. The flame velocity is the same as that shown in Figure 5.2. The vessel pressure grows monotonically to a maximum of about 5.5 times the initial pressure. This is a conservative estimate of vessel pressure because heat transfer from the hot combustion products to the vessel wall is not considered. The time required for the flame to traverse the entire vessel length is about 7 seconds, which allows plenty of time for the gas to cool. The cooling of the hot gases is also a mechanism for decelerating the flame.

The model predictions for flame velocity versus propagation distance in a vented and unvented vessel for a 10 percent hydrogen in air mixture at 300K is given in Figure 5.4. For the venting case, the critical vent cover pressure is taken as 0.1 MPa (i.e., no vent cover clips). The vent section locations are depicted in Figure 5.3 by horizontal lines spanning the active venting length. For the venting case, the flame initially accelerates more rapidly than the case with no venting. This enhanced flame acceleration in the first pipe section, which has also been observed experimentally, is due to the venting of the unburnt gas which in effect pulls the flame forward. Once the flame reaches the first vent section, the flame velocity decreases as a result of venting of the burnt gas. Once the flame emerges from the first vent section, it resumes to accelerate until it reaches the next vent section at which point the flame decelerates once again. After the flame emerges from the second vent section, it is incapable of reaccelerating due to the increased venting of the product gases. Finally, after the third vent section, the flame decays to essentially the laminar burning velocity of the mixture. It is difficult to compare these predictions with the experimental measurements in the slow deflagration regime since in most tests there was an insufficient number of thermocouples to observe such variations in the flame velocity between vent sections (see Figure 4.1).

In summary, the model is successful in predicting two of the experimental observations made in the present venting study; 1) flame acceleration is enhanced by the venting of the unburnt mixture, and 2) flame acceleration is impeded by the venting of the combustion products. The model also successfully predicts that the rate of flame acceleration increases with the hydrogen concentration; however, the model fails to predict the negative effect of the mixture initial temperature on flame acceleration. That is, the model predicts that the flame acceleration increases with initial temperature, which is contrary to the experimental observations. This trend in the rate of flame acceleration with temperature is due to the fact that even though the density ratio across the flame decreases with initial temperature, the corresponding increase in the laminar burning velocity more than compensates.

5.2 Flame Propagation Mechanism in the Choking Regime

In flame acceleration experiments in an obstacle-laden tube without venting, the flame was observed to propagate at a "global" steady-state velocity just below the speed of sound in the burnt gas. The term global is used since locally, between obstacles, the flame velocity is not steady due to gasdynamic effects associated with fluid flow through the orifice plates. This effect is most pronounced for large blockage ratio orifice plates where flame propagation consists of progressive jet initiation of the combustible gas between orifice plates. However, the unsteadiness of the local phenomenon is masked if the average velocity is measured over several obstacles. In flame acceleration in an obstacle-laden tube with lateral venting, flame propagation is unsteady on both a local and to a certain extent a global scale. The present study indicates that flame propagation consists of flame acceleration through the unvented pipe section followed by deceleration through the vent section. In the pipe section, the flame velocity tends to approach the choking velocity observed in unvented tests. However, the acceleration process is moderated by the vent sections so that the average velocity measured over a pipe and vent section can be considerably below the choking velocity.

Insight into the oscillatory nature of the combustion front propagation can be obtained by analyzing the structure of the flame-shock complex. By using the pressure measurements and the photodiode signals, we can determine the structure of the flame-shock wave complex before it enters the vent section and after it passes through the vent section. In the analysis, let us consider a 20 percent

hydrogen in air mixture with 25 percent steam dilution at 650K. As shown in Figure 4.10, flame propagation in this mixture displays the typical characteristics associated with propagation in the choking regime, as described above. The pressure time histories obtained during the tests at a distance of 0.91 meters before and after the last vent section are shown in Figure 4.11. Since the photodiode and the pressure signals are both recorded on a common-time base, we can determine the relative positions of the flame and the various shock waves. Let us consider their positions when the main shock wave, i.e., corresponding to the second pressure rise in Figure 4.11a, arrives at the pressure transducer located before the vent. The pressure ratio across the precursor shock wave is 1.29, which from the normal shock tables yields a shock Mach number of 1.12. From the equilibrium code STANJAN (Reynolds, 1986), the sound speed in the mixture is 574 m/s, which yields a shock wave velocity of 643 m/s. From Figure 4.11a, the time difference between the time of arrival of the precursor shock and the main shock wave at the pressure transducer is 0.65 ms, which means the precursor shock is 42 cm ahead of the main shock. Based on normal shock relations, this precursor shock induces a gas velocity of 108 m/s behind it and increases the speed of sound to 595 m/s. From Figure 4.11a, the pressure ratio across the main shock is 1.7 which yields a shock Mach number and a relative shock wave velocity of 1.27 and 753 m/s, respectively. Taking into account the 108 m/s flow generated by the precursor shock, the velocity of the main shock velocity relative to the vessel is 862 m/s. At the instant the main shock arrives at the pressure transducer, we can infer from the photodiode signals that the flame lags behind at a distance of 62 cm and is propagating at a velocity of 720 m/s. Since the flame is still accelerating at this point, it continues to generate compression waves which overtake and strengthen the main shock. This is substantiated by the fact that the pressure appears to increase with time after the reflected shock (e.g., third pressure rise) in Figure 4.11a.

In a similar fashion, we can analyze the flame-shock structure after it emerges the last vent section. The pressure ratio across the first shock wave in the pressure trace shown in Figure 4.11b is 1.65, which corresponds to a shock Mach number of 1.25, and taking the speed of sound in the unburnt gas to be 574 m/s, this yields a shock wave velocity of 718 m/s. The pressure drop after the initial pressure jump indicates that the shock wave is actually a decaying blast wave. From the photodiode signals, we can infer that the flame is 115 cm behind the shock wave when the shock reaches the pressure transducer. The second detectible pressure rise which corresponds to a shock wave occurs 1 m/s after the initial shock wave. This time corresponds to a separation distance of 72 cm which places it between the initial shock wave and the flame.

Figure 5.5 schematically shows the relative positions and velocities of the shock waves and the flame both before and after the last vent section as calculated above. From this figure, a clear picture of the interaction between the shock-flame complex and the vent section emerges. Since this interaction occurs between each vent section, the details of the shock-flame complex shown after Vent Section 4 also applies after Vent Section 3, and thus a complete description of the phenomenon between vents can be put together.

As shown in the top schematic of Figure 5.5, by the time the flame reaches half way through the straight pipe section before the vent, the main shock wave is 62 cm ahead. Taking a constant main shock velocity of 862 m/s, the time required for it to overtake the precursor shock is 1.92 ms. In this amount of time, the precursor shock wave propagates a distance of 1.23 meters which is farther than the 0.8 meter distance to the vent section. In reality, since the main shock wave is strengthening and thus its velocity is increasing, the distance required for it to overtake the precursor shock will be

shorter. Whether or not the two shock waves merge before entering the vent section will depend on the increase in the main shock velocity, which in turn is governed by the rate of flame acceleration. In any case, if the precursor shock wave arrives first at the vent section, the severe wave diffraction will cause it to slow down and most likely merge with the main shock wave. The blast wave that emerges from the vent section (see bottom of Figure 5.4) is the remnant of the main shock wave along with the precursor shock.

As the main shock wave and the flame propagate through the vent section, their respective velocities are reduced, and they decouple causing the distance between them to almost double compared to before the vent section. As the flame emerges from the vent section into the straight pipe section, the lateral confinement within the pipe section allows the flame to reaccelerate. The flame acceleration produces a new main shock which strengthens via compression waves generated by the flame. This new main shock wave then chases the precursor shock wave which had formed from the decaying original main shock wave that earlier had passed through the vent section.

An important finding in the present experiments is that once the flame has accelerated to a velocity on the order of the product gas sound speed, venting as provided by the HTCF, becomes ineffective in dampening the flame to a benign state. In the choking regime, flames, on the average, move at roughly the speed of sound in the products. Rarefaction waves, produced in the venting of the burnt gas, cannot then overtake the flame to slow it down. The pressures associated with deflagrations in the choking regime can be quite high (e.g., on the order of the AICC pressure).

5.3 Propagation in the Detonation Regime

In flame acceleration tests performed in nonvented obstacle-laden tubes, transition to detonation occurred after a certain run-up distance (Ciccarelli et al., 1996) if the mixture detonation cell size, λ, was smaller than the orifice plate opening, d. This experimental observation lead to the DDT limit criterion $d/\lambda = 1$, used to identify the minimum hydrogen concentration required for transition to detonation. If the run-up distance is longer than the tube length, transition to detonation cannot occur, even if the DDT limit criterion is met. As described in the previous section, the flame acceleration process is interrupted by a vent section whereby the flame velocity drops by up to 30 percent across the vent. This process of acceleration in the straight sections and deceleration in the vent sections continues as long as there are vent sections ahead of the flame. In order for flame acceleration to result in transition to detonation in a multiple vented tube, not only should the DDT limit criterion be met, but also there must be sufficient distance between the vents for the flame to accelerate to a point where DDT can occur. As can be seen in Tables 4.1 and 4.2, for the minimum hydrogen concentrations where DDT was observed, the d/λ value was about 6 and even as high as 11.9 for the dry hydrogen-air mixtures at 650K. This indicates that the vents are effective in limiting the possibility of transition to detonation over and above the well-known effect of the orifice inner diameter. If the spacing between vent sections was reduced, the value of d/λ corresponding to the minimum hydrogen concentration where DDT occurs would probably increase. Of course, the opposite would be true if the vent spacing was increased. The value of d/λ at the limit would decrease approaching a value of unity corresponding to the unvented case. Therefore, most likely, there is a minimum vent spacing required for the vents to be effective in mitigating DDT.

In those mixtures where DDT occurred, the detonation eventually failed (i.e., shock wave and reaction zone decouple) at a vent section further down the vessel. The detonation fails at the vent section as

a result of shock diffraction. It is well known that a minimum number of detonation cells is required for a detonation wave to propagate from a tube into an unconfined geometry. This is referred to as the critical tube phenomenon. For most mixtures, at least 13 cells are required for successful transmission; however, for mixtures displaying a regular cellular pattern, up to 26 cells are required (Desbordes et al., 1993). Note, in the present experiments, the orifice plates continue through the vent sections so a direct analogy with the critical tube phenomenon cannot be made. However, one would expect that the orifice plates provide a surface for shock reflection which would aid in the reinitiation of the failing detonation wave and thus result in a critical d/λ lower than 13. In the present experiments, all the mixtures which resulted in transition to detonation had less than 13 cells across the orifice inner diameter. In none of the mixtures tested did a detonation wave propagate through the entire vessel; as such, we, therefore, cannot comment on this critical condition. Further experiments with more sensitive mixtures are required to explore this issue.

5.4 Applications to Reactor Safety

As discussed in the Introduction, hypothetically, a plausible mechanism for detonation initiation in a nuclear power plant environment is via flame acceleration. In a nuclear power plant, the greatest probability for flame acceleration leading to the onset of a detonation is in long narrow compartments or corridors which may have turbulence-inducing obstacles, such as pumps, cables, etc. In most cases, these compartments also have vent paths, such as doors and air ducts, which can hamper the ability of a flame to accelerate. Therefore, it is worthwhile to look into the effect of venting on flame acceleration and DDT. The difficult question is what venting geometry to use in the study. If one is interested in a particular compartment in a power plant, one might design a scaled-down model to perform the tests. That was the approach taken in the venting experiments carried out in the FLAME Facility at Sandia (Sherman et al., 1989), where the channel is a half-scale model of the upper plenum region of an ice-condenser containment. If this is not the case, clearly, there is no one geometry which can be used to describe all the possible vent configurations which might exist in the power plant. Therefore, one should design the experiment under the most ideal conditions and study the effects of various parameters. This was the philosophy behind the DDT tests without venting performed in the past and with venting in the present study.

Experiments carried out without venting indicated that the DDT limit criterion of $d/\lambda = 1$ was a necessary but not sufficient condition to predict the possibility of transition to detonation (Ciccarelli et al., 1996). In particular, the DDT limit criterion was shown to be conservative in the case of DDT in hydrogen-air mixtures at 650K because of the inability, at these temperatures, for lean mixtures to support flame acceleration. The experimental findings from the present study indicate that the vents used in the HTCF have a strong effect on the ability of the flame to accelerate and undergo transition to detonation in the vent configuration tested. In general, it has been observed that DDT occurred after the flame entered the cyclic velocity pattern characteristic of the choking regime. In order for DDT to occur, the flame must accelerate to a velocity on the order of the speed of sound in the products (e.g., choking). Clearly, if venting prevents flame acceleration to such velocities, DDT can be ruled out.

To evaluate the possibility of DDT in a particular compartment geometry, one can use the DDT limit criterion in conjunction with detonation cell size data for the expected mixture composition. This must be considered a conservative approach since no consideration is given to the process by which the detonation is initiated. In the case of DDT, one is assuming that conditions in the compartment are favorable for flame acceleration. Experimentally, it has been shown that both venting and the mixture

initial temperature play important roles in mitigating flame acceleration and thus transition to detonation. In the case of the effect of venting, the results are absolutely apparatus dependent, and, therefore, it is difficult to incorporate the experimental results directly into an analysis dealing with DDT phenomenon in realistic geometries. Since no simple criterion exists, a capability for performing numerical simulations of the gas dynamics behavior of accelerating flames through and within actual vented compartment configurations will be helpful. Sensitivity studies can then be performed to investigate select geometric/thermodynamic/chemical kinetic parameters on the overall process. Such a numerical, computational fluid dynamics code presently does not exist. Of course, this code must first be benchmarked with experimental data on flame acceleration with and without venting. The data obtained in this investigation are ideal for such an exercise. Although modeling of DDT phenomenon is not possible even with state-of-the-art combustion codes, one can still look at the effect of venting on the ability of the flame to accelerate to velocities on the order of the speed of sound in the products.

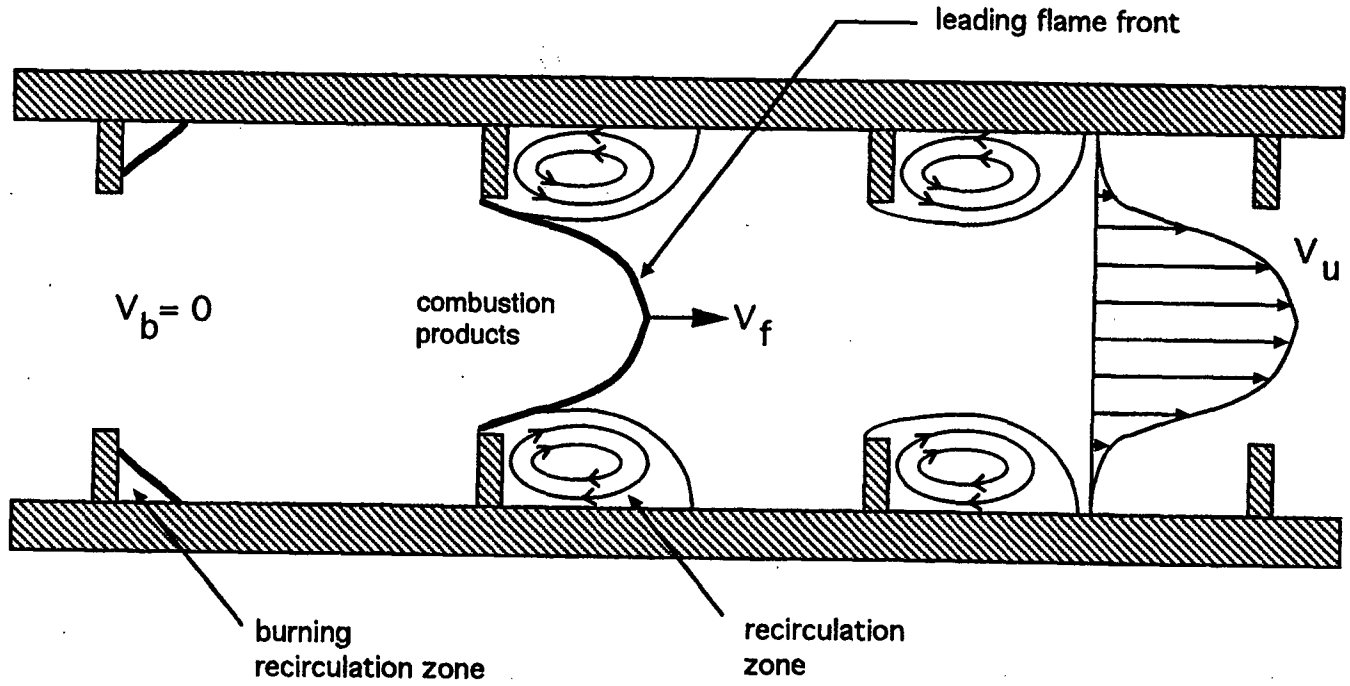

Figure 5.1 Schematic of the assumed flame structure in the non-vented tube section

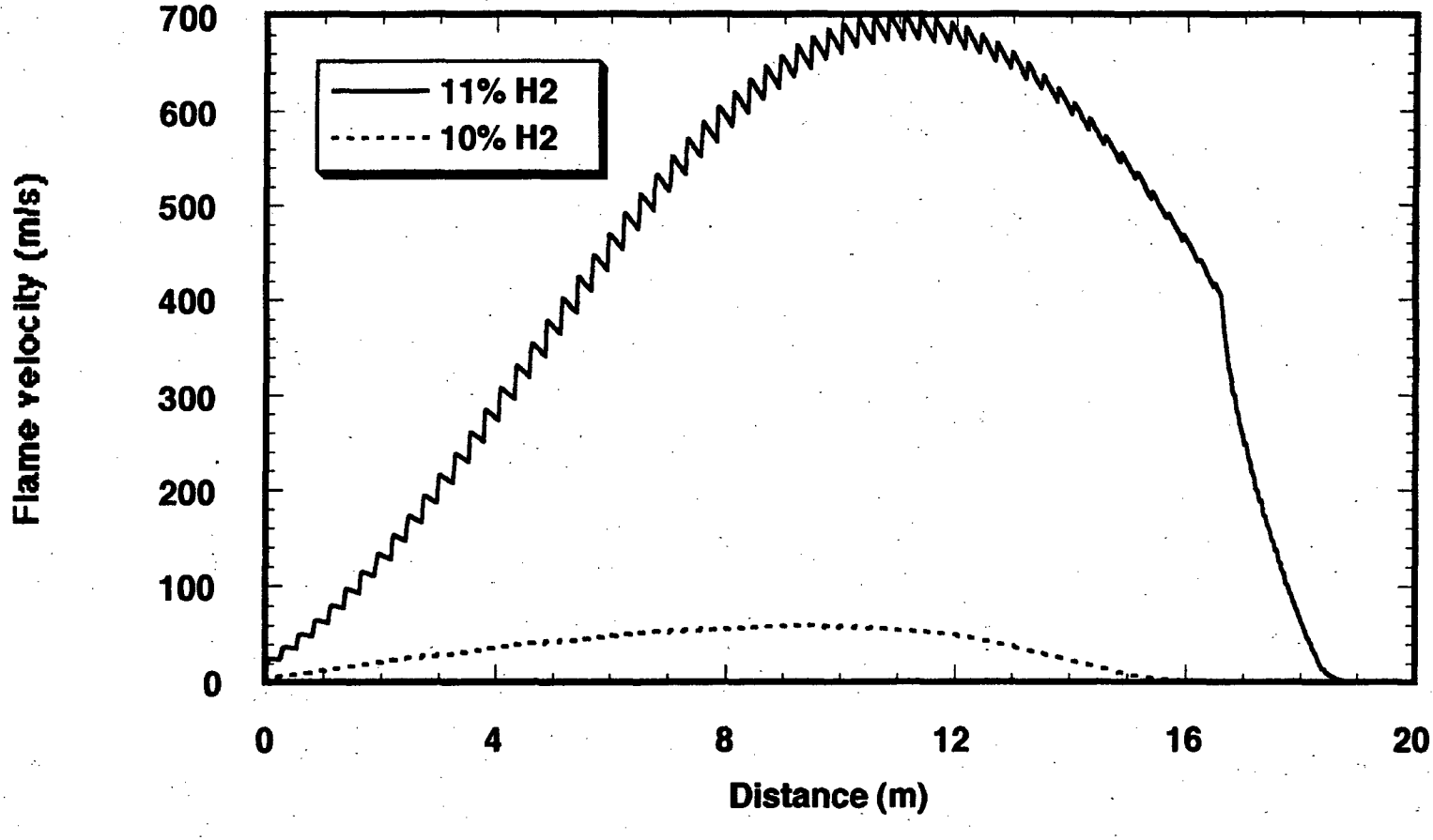

Figure 5.2 Model prediction of flame velocity versus distance for 10 and 11 percent hydrogen in air mixtures at 300K

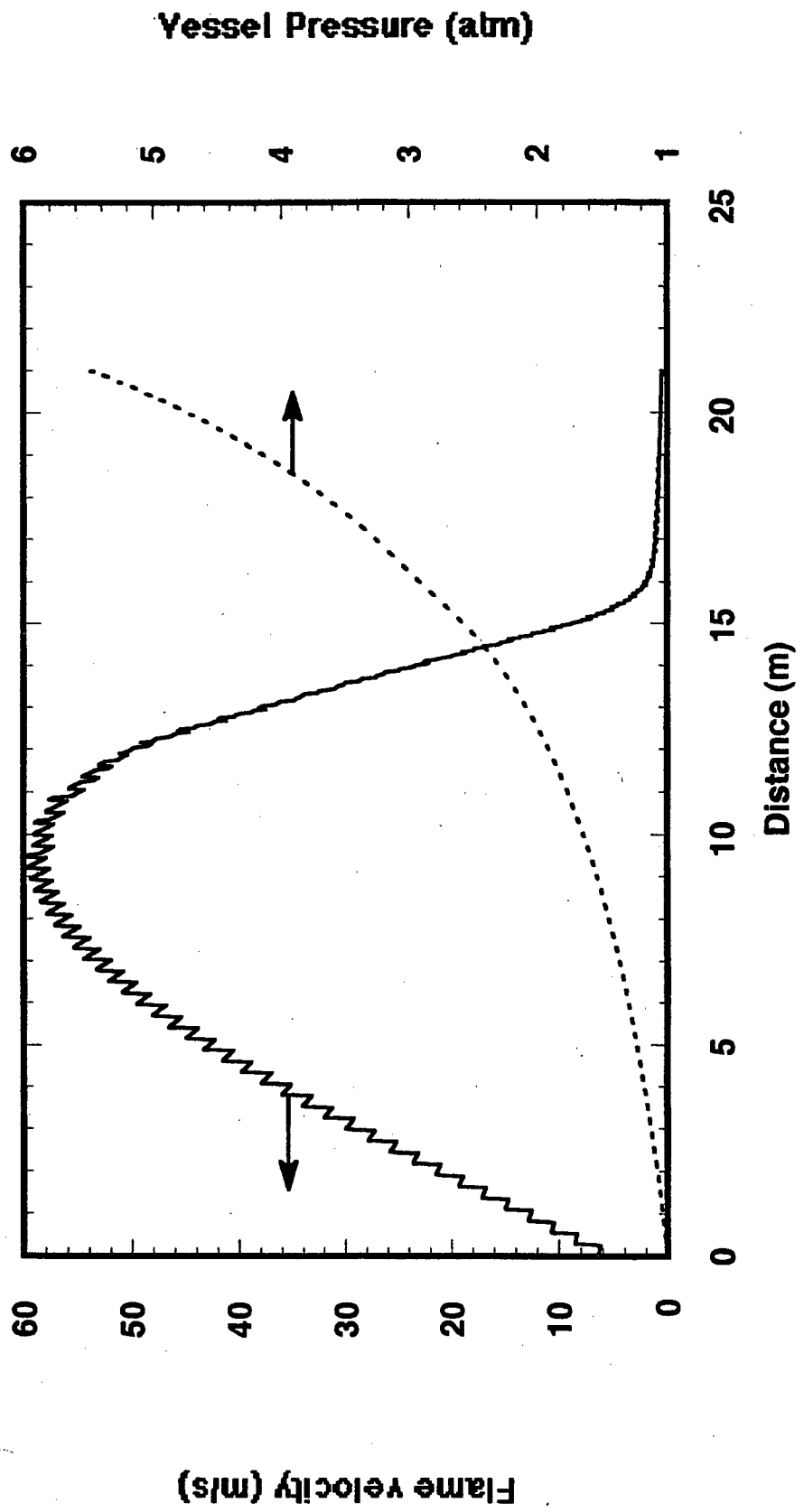

Figure 5.3 Model predictions of flame velocity and vessel pressure versus distance for a 10 percent hydrogen in air mixture at 300K

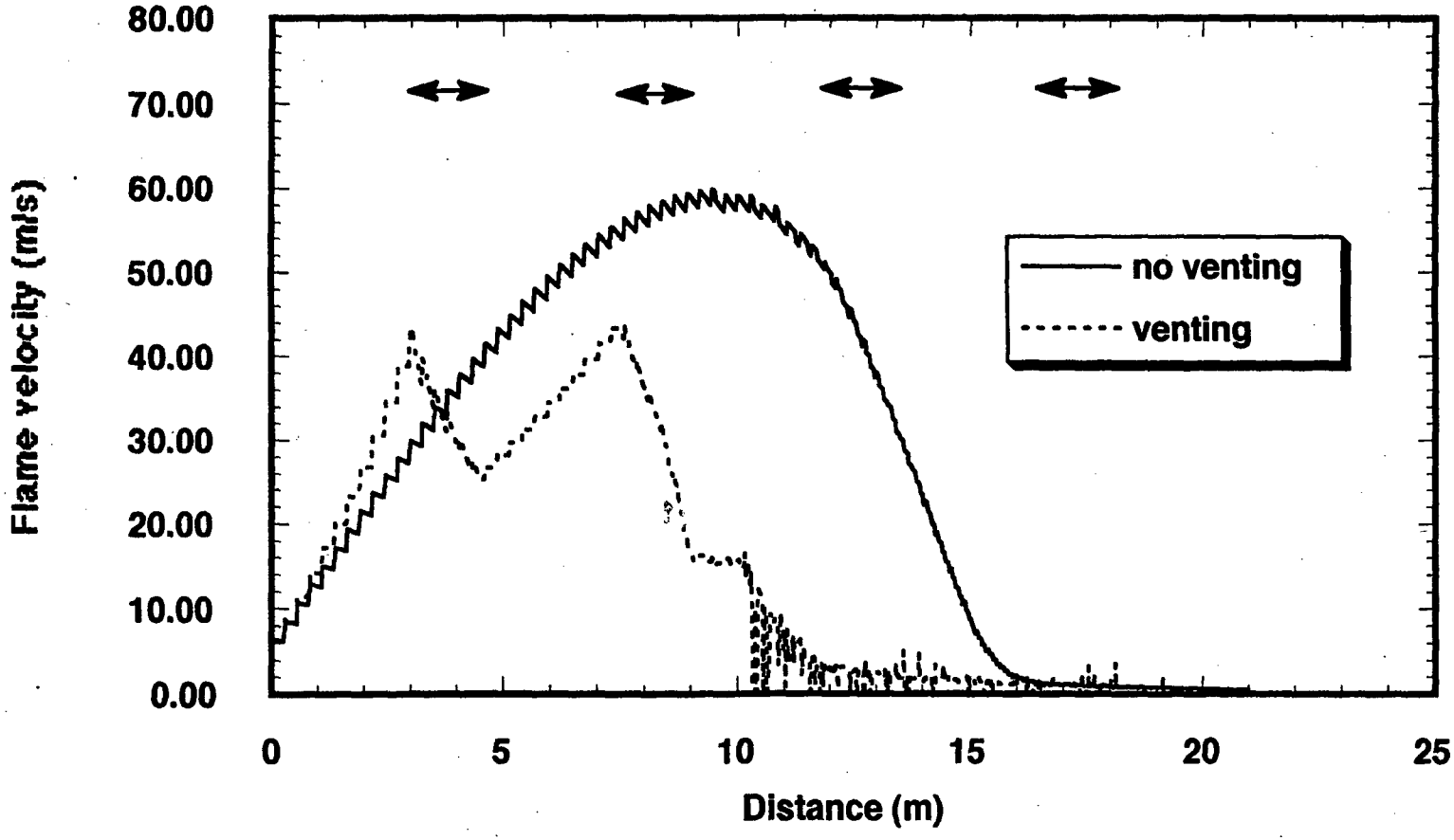

Figure 5.4 Model prediction of flame velocity versus distance for a 10 percent hydrogen in air mixture at 300K, with and without venting

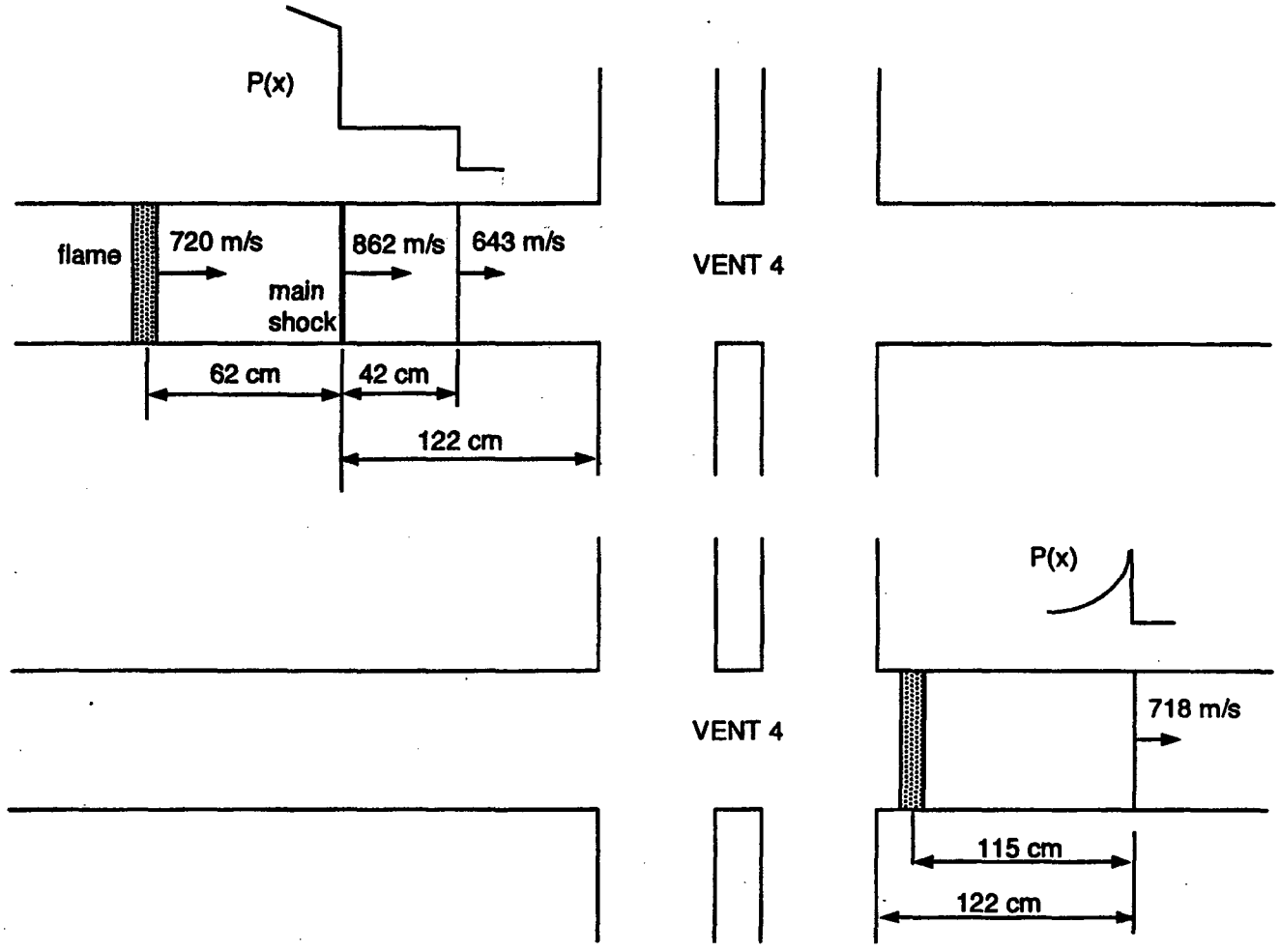

Figure 5.5 Flame-shock structure before and after the last vent section for flame propagation in the choking regime (e.g., 20 percent hydrogen in air mixture with 25 percent steam dilution)

6. CONCLUSIONS

The present report describes the results obtained in the study of the influence of venting on flame propagation in an obstacle-laden tube. The experiments were carried out in the HTCF equipped with orifice plates with a 1-tube-diameter spacing and blockage ratio of 0.43. The four vent sections, each with four vent openings with areas equal to the vessel cross-sectional area, were located between straight pipe sections. This corresponds to a total vent area of 5.1 percent of the total vessel surface area. The parameters in the experiments are the mixture initial temperature (up to 650K) and the mixture composition. The tests were performed in dry and steam-diluted hydrogen-air mixtures. In general, for the test apparatus configuration studied, venting reduced the likelihood of DDT at all initial temperatures.

As was the case in the flame acceleration tests without vents, after an initial flame acceleration phase, the flame would either a)decay, b) reach a quasi-steady velocity on the order of the speed of sound in the burnt gas, or c) for a limited number of tests with sensitive mixtures, accelerate and lead to the onset of a detonation wave. These propagation regimes could be classified as:

(a) Slow Deflagrations: In this regime, the flame accelerates to a maximum velocity of about 100-200 m/s and then decelerates to a velocity on the order of meters per second. No significant pressure is generated in this propagation regime. A simple venting model was developed to demonstrate the effect of venting burnt and unburnt gases on flame acceleration.

(b) Choking Regime: Flame acceleration is followed by an oscillatory propagation mode where the flame accelerates in the tube section and decelerates across the vent section. The mean flame velocity is just under the speed of sound in the burnt products. The structure of the combustion front consists of a turbulent flame preceded by a weak precursor shock wave and a stronger leading shock wave. The leading shock wave is generated ahead of the turbulent flame and has a typical pressure rise just under the AICC pressure. The weak wave is generated by the decoupling of the leading shock wave and the flame in the vent section. Therefore, the weak precursor wave is a product of the leading shock wave after it emerges from the vent section.

(c) Detonation Regime: In particularly sensitive mixtures, a detonation wave was initiated. In all the cases studied, the detonation wave failed before the end of the vessel as a result of wave diffraction in the vent section. One would expect if the mixture cell size is small enough, a detonation wave could propagate through the entire vessel unimpeded by the orifice plates and the venting.

The influence of venting on the combustion phenomenon could be measured by the change in the choking and the DDT limits measured compared to the tests without venting. The choking limit, which is in effect the minimum hydrogen composition where significant flame acceleration takes place, increased for all initial temperatures and steam dilution in the experiments with venting. For example, for dry hydrogen-air at 500K, the choking limit in the no venting experiments was 8 percent hydrogen, whereas this limit increased to 11 percent hydrogen in the venting experiments. At 650K, the choking limit increased by 2 percent hydrogen for both dry and 25 percent steam-diluted hydrogen-air mixtures. The effect of venting was less pronounced at the lower temperatures. At 300K, the choking limit in dry hydrogen-air only increased by 1 percent hydrogen, and at 400K with 10 percent steam, the choking limit was unchanged at 12 percent hydrogen.

6. Conclusions

The DDT limit, which in this case is defined as the minimum hydrogen composition where a detonation is observed, like the choking limit was also affected by venting. For example, for hydrogen-air mixtures at 500K the DDT limits increased from 12 percent hydrogen with no venting to 15 percent hydrogen with venting. The study without venting had shown that for hydrogen-air mixtures at 500K the DDT limit criterion was $d/\lambda = 1$. In the present study with venting, for hydrogen-air mixtures at 500K, the DDT limit is $d/\lambda = 5.5$.. At an initial temperature of 650K, the DDT limit increased from 11 percent hydrogen ($d/\lambda = 8$) with no venting to 13 percent hydrogen ($d/\lambda = 12$) in the tests with venting.

To evaluate the possibility of DDT on a nuclear power plant scale for the purpose of severe-accident analysis, the best one can do is to use the $d/\lambda = 1$ DDT limit criterion in conjunction with detonation cell size data for the expected mixture composition. This can be considered a conservative approach since no consideration is given to the process by which the detonation is initiated. In the case of DDT, one is assuming that conditions in the compartment are favorable for flame acceleration. Experimentally, it has been shown that both venting and the mixture initial temperature play important roles in flame acceleration. In experiments without venting, it was shown that for higher initial temperatures, the ability of the flame to accelerate, as quantified by the run-up distance, was reduced even though the mixture sensitivity to detonation increased, as measured by a decrease in the detonation cell size. In the present study, it has been shown that 5% venting also limits the flames ability to accelerate. Since venting has no affect on the detonation cell size, which is a fundamental property of the mixture, it is considered a strong mitigating effect on DDT. It should be stressed that the results are absolutely apparatus dependent, both geometric and scaling effects should be taken into account when studying flame acceleration at much larger scales or with a different vent area configuration.

7. REFERENCES

Alexiou, A., H. Phylaktou, and G. Andrews, "The Effect of Vent Size on Pressure Generation During Explosions in Large L/D Vessels," Presented at the 15th International Colloqium of Explosions and Reactive Systems, Colorado, 1995.

Beauvais, B., F. Mayinger, and G. Strube, "Severe Accident in a Light Water Reactor: Influence of Elevated Initial Temperature on Hydrogen Combustion," ASME/JSME Nuclear Engineering Conference-Volume 1, pp. 425-433, 1993.

Bradley D., and A. Mitcheson, "The Venting of Gaseous Explosions in Spherical Vessels, Part II-Theory and Experiment," Combustion and Flame 32, pp. 237-255, 1978.

Chan, C., D. Lau, and D. Radford, "Transition to Detonation from Burning in a Confined Vortex," Proceedings of the 22nd Symposium (International) on Combustion, Combustion Institute, 1989.

Chan, C., I. Moen, and J.H. Lee, "Influence of Confinement on Flame Acceleration Due to Repeated Obstacles," Combustion and Flame 49, pp. 27-39, 1983.

Ciccarelli, G., et al., "The Effect of Initial Temperature on Flame Acceleration and Deflagration-to-Detonation Transition Phenomenon," NUREG/CR-6509, BNL-NUREG-52515, 1998.

Cooper, M., M. Fairweather, and J. Tite, "On the Mechanism of Pressure Generation in Vented Explosions," Combustion and Flame 65, pp. 1-14, 1986.

Desbordes, D., et al., "Failure of the Classical Dynamic Relationships in Highly Regular Cellular Detonation Systems," Progress in Astronautics and Aeronautics, 153, pp. 347-359, 1993.

Guirao, C., R. Knystautas, and J. Lee, "A Summary of Hydrogen-Air Detonation Experiments," NUREG/CR-4961, SAND87-7128, 1989.

NFPA 68, "Guide for Venting of Deflagrations," National Fire Protection Association, Quincy, 1994.

Rabash, D., and Z. Rogowski, "Gaseous Explosions in Vented Ducts," Combustion and Flame, 4, pp. 301-312, 1960.

Sherman, M., S. Tieszen, and W. Benedick, "FLAME Facility: The Effect of Obstacles and Transverse Venting on Flame Acceleration and Transition to Detonation for Hydrogen-Air Mixtures at Large Scale," NUREG/CR-5275, SAND85-1264, 1985.

Solberg, D., and J. Pappas, "Observation of Flame Instabilities in Large-Scale Vented Gas Explosions," Proceedings of the 18th Symposium (International) on Combustion, Combustion Institute, 1981.

Tite, J., T. Binding, and M. Marshall, "Explosion Reliefs for Long Vessels," Fire and Explosion Hazards, The Institute of Energy, 1991.

APPENDIX A

TABULATED DATA

The following table provides a summary of all the experiments performed in this test series. All tests were performed at an initial pressure of 0.1 MPa. The data is grouped in terms of tests performed at common initial temperatures with and without steam dilution. In all cases, the quoted initial temperature has an uncertainty of ±14K which corresponds to the measured temperature uniformity from thermal calibration tests performed on the vessel. The hydrogen concentration, reported on a dry basis, is obtained from gas samples taken from the vessel prior to ignition and analyzed using a gas chromatograph. For each test, three gas samples were taken from the vessel covering the entire length of the vessel. For each sample bottle, typically two samples were run through the gas chromatograph. Shown in the table is the average and the standard deviation of these six samples. The steam dilution reported is a nominal value obtained from the set venturi constituent flow rates; no direct measurement of the steam dilution was made. The last column indicates the mode of propagation observed for each respective test.

Table A.1 Summary of initial thermodynamic conditions for each test

Test No.	Temperature (K)	Hydrogen (%) Average	SDV	H_2O (%)	Propagation Mode
12	300	9.07	0.02	0	slow deflagration
13	300	9.85	0.03	0	slow deflagration
14	300	10.88	0.07	0	slow deflagration
15	300	12.12	0.07	0	choking
22	500	10.25	0.02	0	slow deflagration
16	500	10.31	0.03	0	slow deflagration
23	500	11.09	0.03	0	choking
17	500	11.23	0.04	0	choking
33	500	11.32	0.03	0	choking
46	500	12.85	0.07	0	choking
47	500	14.67	0.05	0	choking
48	500			0	detonation
02	650	11.08	0.02	0	slow deflagration
21	650	12.22	0.06	0	slow deflagration
04	650	12.97	0.11	0	choking
20	650	13.22	0.11	0	choking
30	650	13.20	0.19	0	detonation
05	650	13.91	0.06	0	detonation
01	650	14.74	0.16	0	detonation
08	650	27.09	0.13	*	detonation

Test No.	Temperature (K)	Hydrogen (%) Average	SDV	H_2O (%)	Propagation Mode
27	400	10.38	0.04	10	slow deflagration
26	400	11.11	0.02	10	slow deflagration
40	400	12.04	0.05	10	choking
41	400	12.66	0.08	10	choking
24	500	14.23	0.04	25	slow deflagration
19	500	14.22	0.04	25	slow deflagration
18	500	14.54	0.09	25	no good
11	500	15.03	0.02	25	choking
32	500	15.35	0.03	25	choking
34	500	16.70	0.01	25	choking
37	500	19.78	0.03	25	choking
38	500	21.67	0.09	25	choking
06	650	15.85	0.27	25	slow deflagration
28	650	17.53	0.03	25	slow deflagration
07	650	17.75	0.07	25	slow deflagration
10	650	17.96	0.07	25	choking
29	650	18.38	0.06	25	choking
31	650	18.95	0.15	25	choking
36	650	19.32	0.11	25	choking
44	650	19.69	0.02	25	choking
43	650	21.45	0.02	25	choking
42	650	21.50	0.28	25	choking
45	650	22.88	0.07	25	detonation

* unknown quantity

APPENDIX B

In this section, the model used to describe flame propagation in the slow deflagration regime will be described. This model is an extension of the model proposed by Chan et al. (1983), and the derivation of the governing equations will follow very closely their approach. A schematic of the flame structure used in the model is given in Figure B.1. From conservation of mass, the rate of increase in the mass of burnt gas due to combustion is equal to the rate of change of mass of burnt gas in the vessel plus the rate at which burnt gas is vented,

$$dm_b/dt = d(\rho_b V_b)/dt + dm_{vb}/dt \qquad \text{B.1}$$

where V_b is the total volume occupied by the burnt gas, ρ_b is the burnt gas density, and $d(m_{vb})/dt$ is the rate at which burnt gas is vented. The total rate of increase of mass of burned gas due to combustion includes a term from the flame front in the mainstream and the burning of the gas in the recirculation zone

$$dm_b/dt = \rho_u A_f S_f + \rho_u dV_c/dt \qquad \text{B.2}$$

where A_f is the main flame area, S the main flame burning velocity, and dV/dt is the volumetric burning rate in the recirculation zone. Combining Equations B.1 and B.2 and assuming isentropic compression of the burnt gas, one gets

$$\rho_b dV_b/dt + (\rho_b V_b/\gamma_b P)dP/dt + dm_{vb}/dt = \rho_u A_f S_f + \rho_u dV_c/dt \qquad \text{B.3}$$

where P is pressure and γ_b is the ratio of the specific heats in the burnt gas. The time rate of change of the gas volume, dV_b/dt, can be expressed as

$$dV_b/dt = A_f dR_f/dt + dV_c/dt \qquad \text{B.4}$$

where dR_f/dt is the flame velocity. The burning of the gas in the recirculation zone involves the entrainment of the flame and the subsequent burnout of the gas. A rigorous model for this phenomenon is beyond the scope of this model; instead we will assume a constant volumetric burning rate for the gas in the recirculation zone

$$dV_c/dt = V_c/\tau = V_c/(V_c^{1/3}/S_c) = V_c^{2/3}/S_c \qquad \text{B.5}$$

where τ is the characteristic burnout time and V_c is the volume of the recirculation zone. Note for time later than τ, the burning rate is zero. The burnout time is taken as the characteristic length scale of the recirculation zone (i.e., $V_c^{1/3}$) divided by the burning velocity, S_c. Combining Equations B.3, B.4, and B.5, we can obtain the following expression for the flame velocity

$$dR_f/dt = (\rho_u/\rho_b)S_f + (\rho_u/\rho_b - 1)V_c^{2/3}/S_c A_f - (\rho_b V_b/\gamma_b P A_f)dP/dt - (1/A_f \rho_b)dm_{vb}/dt \qquad \text{B.6}$$

The first two terms in Equation B.6 are always positive and so they promote flame acceleration. The third term governs the compression and expansion of the burnt gas. This term is positive if the pressure is increasing and thus it has a retarding effect on the flame, and if the pressure is decreasing,

this term promotes flame acceleration. The last term represents the retarding effects of venting the burnt gas.

A similar control volume analysis can be performed on the unburnt gas to yield the following relationship for the flame velocity

$$dR_f/dt = S_f + (V_o - V_b)/\gamma_u P A_f \, dP/dt - (1/A_f \rho_u) dm_{vu}/dt \qquad B.7$$

where V_o is the volume of the vessel and dm_{vu}/dt is the rate at which unburnt gas is vented ahead of the flame. By rearranging Equation B.7, the following expression for the rate of change in pressure can be obtained

$$dP/dt = \gamma_u P A_f /(V_o - V_b)(dR_f/dt - S_f) - (\gamma_u P/\rho_u) dm_{vu}/dt \qquad B.8$$

By replacing dP/dt in Equation B.6 by the expression in Equation B.8 yields an expression for the flame velocity independent of dP/dt. Given expressions for the respective vent mass flow rates, for the burning velocity, and the volume of the recirculation zone, we have two unknowns (i.e., flame velocity and vessel pressure) and two equations which can be solved simultaneously.

Vent Mass Flow Rate and Vent Cover Motion

The vent mass flow rate, based on the flow through an orifice, is given by

$$\frac{dm_{vu}}{dt} = \rho c A_v C_D \left[\frac{2}{\gamma - 1} \left(\frac{P_o}{P} \right)^{\frac{2}{\gamma}} \left(1 - \left(\frac{P_o}{P} \right)^{\frac{\gamma - 1}{\gamma}} \right) \right]^{\frac{1}{2}} \qquad p < P_c$$

and

$$\frac{dm_{vu}}{dt} = \rho c A_v C_D \left[\left(\frac{2}{\gamma + 1} \right)^{\frac{\gamma + 1}{\gamma - 1}} \right]^{\frac{1}{2}} \qquad p > P_c$$

where P_o is the atmospheric pressure, C is the speed of sound in the gas, A_v is the vent area, and C_D is the discharge coefficient which is taken to be 0.7. The critical pressure, P_c, is given by

$$P_c = P_o \left(\frac{\gamma + 1}{2} \right)^{\frac{\gamma}{\gamma - 1}}$$

which for $\gamma = 1.4$ yields a critical pressure of 1.9 times atmospheric pressure. There are two vent mass flow rates which appear in the equations to be integrated: one for the unburnt gas ahead of the flame and one for the burnt gas behind the flame. The value of A_v takes on different values during the calculation depending on the position of the flame. At the start of the calculation, A_v for the burnt gas is zero and A_v for the unburnt gas is $4\pi D^2$, i.e., there are four vent sections each with four vent openings equal to the cross-sectional area of the main tube. After the flame passes the first vent, A_v for burnt gas takes on a value of πD^2 and A_v for the unburnt gas takes on a value of $3\pi D^2$. As the

flame propagates through the vent, the fraction of the vent area which is allocated to the burnt and unburnt gas is proportional to the fraction of the vent axial distance covered by the flame.

In the model, one can assume that the vent covers have mass or are massless. If the vent covers are massless, the covers open immediately upon the start of the calculation. If the mass of the covers are considered, Newton's first law is used to calculate the vent area as a function of time. The acceleration of the vent cover, a_c, is given by the following expression

$$a_c = (P-P_o)(A_c/M_c) \pm g \qquad \text{B.12}$$

where P_o is the pressure outside of the vessel (typically 0.1 MPa), M_c is the cover mass, and g is gravitational acceleration (9.81 m/s^2). The top covers move opposite gravity and thus the negative sign in Equation B.12 applies, and for the bottom covers, the positive sign applies. Integrating Equation B.12 yields the vent cover displacement $h_c(t)$ which is calculated at each time step. The vent area, A_v, for each vent opening is thus $\pi D h_c(t)$ until the vent cover has moved a distance D/4 after which the vent area per opening remains $\pi D^2/4$ indicating that the vent cover is fully open.

Burning Velocities

Two burning velocities have been introduced which must be defined in order to integrate the above equations. The ratio of the turbulent burning velocity and the mixture laminar burning velocity, S_L, can be given by an empirical expression involving the mainstream flow velocity, U, ahead of the flame and the rms fluctuation velocity, u'. Following the assumption made by Chan et al. (1983), we will take the ratio of the turbulent burning velocity and the laminar burning velocity to be simply proportional to U, yielding the following simple expression

$$S/S_L = 1 + cU \qquad \text{B.13}$$

where c is a constant. Once the flame velocity is calculated, the effective flow velocity ahead of the flame can be obtained from the following expression

$$U = dR_f/dt\ (\rho_u/\rho_b - 1)/(\rho_u/\rho_b) \qquad \text{B.14}$$

In order to have more flexibility, the burning velocity of the flame in the mainstream, S_f, and the burning velocity used to calculate the burning rate in the recirculation zone, S_c, can take on different values. It is assumed that the burning velocity in the recirculation zone is proportional to the mainstream flow velocity, U, when the flame reaches the obstacle upstream of the recirculation zone. Therefore, the two burning velocities are distinguished by using two different constants in Equation B.13. For example, for the main flame, the constant is c_f, and in the recirculation zone the constant is c_c.

The volume of the recirculation zone is taken to be

$$V_c = \pi(D^2-d^2)c_3(D-d)/8 \qquad \text{B.15}$$

where D is the tube inner diameter and d is the orifice inner diameter. The constant c_3 is a free parameter which gives the ratio of the length of the recirculation zone and the height of the obstacle. Realistic values for c_3 lie in the range 1-5. In order to conserve mass, the mainstream flame area, A_f, is obtained from the following expression

$$\pi(D^2-d^2)c_3(D-d) = (\pi D^2-A_f)D \qquad \text{B.16}$$

where the obstacle spacing is taken to be equal to the tube dimater D.

The density of the unburnt gas is obtained from the chemical equillibrium code STANJAN, and the density of the burnt gas is calculated using STANJAN assuming a constant pressure burn. The laminar burning velocity for the hydrogen-air-steam mixture is obtained from Liu and MacFarlane (1983).

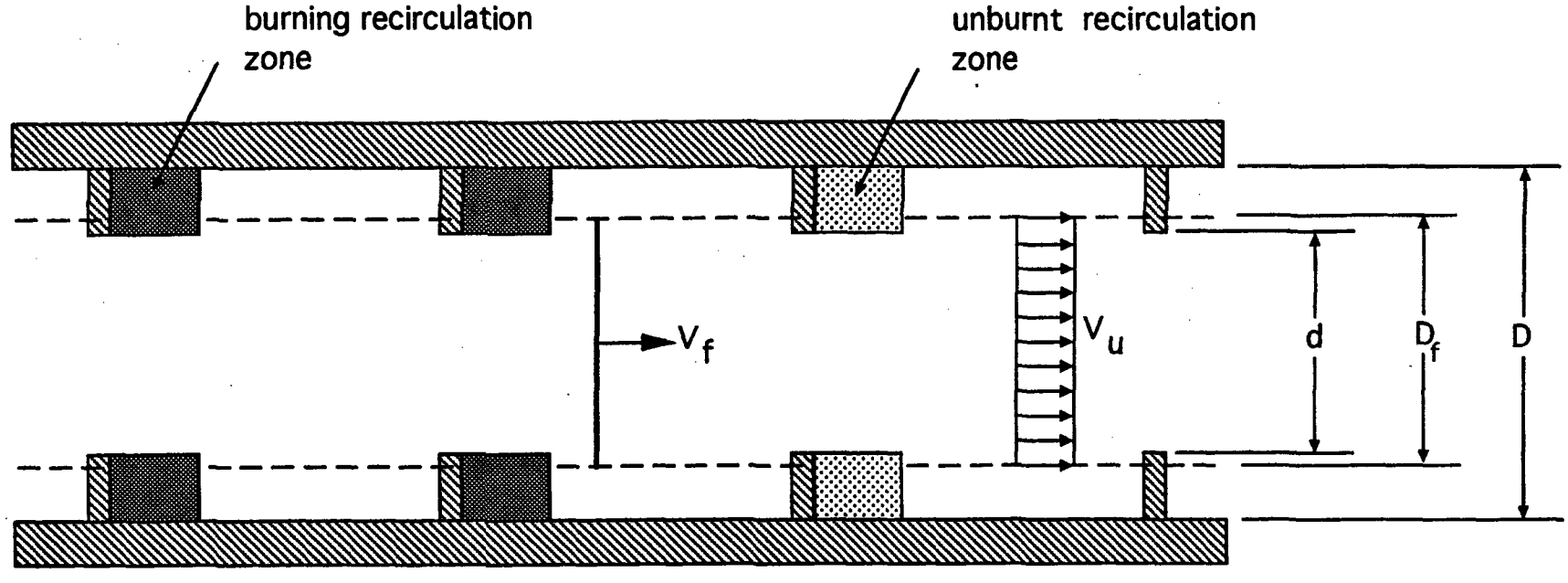

Figure B.1 Schematic showing the assumed flame structure used in the flame acceleration model

NRC FORM 335 (2-89) NRCM 1102, 3201, 3202

U.S. NUCLEAR REGULATORY COMMISSION

BIBLIOGRAPHIC DATA SHEET

(See instructions on the reverse)

1. REPORT NUMBER (Assigned by NRC, Add Vol., Supp., Rev., and Addendum Numbers, if any.)

NUREG/CR-6524
BNL-NUREG-52518

2. TITLE AND SUBTITLE

The Effect of Lateral Venting on Deflagration-to-Detonation Transition in Hydrogen-Air-Steam Mixtures at Various Initial Temperatures

3. DATE REPORT PUBLISHED

MONTH	YEAR
November	1998

4. FIN OR GRANT NUMBER

L1924/A3991

5. AUTHOR(S)

G. Ciccarelli, J. L. Boccio, T. Ginsberg, C. Finfrock, and L. Gerlach, BNL
H. Tagawa, NUPEC
A. Malliakos, US NRC

6. TYPE OF REPORT

Technical

7. PERIOD COVERED *(Inclusive Dates)*

8. PERFORMING ORGANIZATION - NAME AND ADDRESS *(If NRC, provide Division, Office or Region, U.S. Nuclear Regulatory Commission, and mailing address; if contractor, provide name and mailing address.)*

Dept. of Advanced Technology
Brookhaven National Laboratory
Upton, NY 11973-5000

Nuclear Power Engineering Corporation
5F Fujita Kanko Toranomon Building
3-17-1, Toranomon, Minato-Ku
Tokyo 105 Japan

Office of Nuclear Regulatory Research
U.S. Nuclear Regulatory Commission
Washington, DC 20555-0001

9. SPONSORING ORGANIZATION - NAME AND ADDRESS *(If NRC, type "Same as above"; if contractor, provide NRC Division, Office or Region, U.S. Nuclear Regulatory Commission, and mailing address.)*

Division of Systems Technology
Office of Nuclear Regulatory Research
U.S. Nuclear Regulatory Commission
Washington, DC 20555-0001

10. SUPPLEMENTARY NOTES

A. Malliakos, NRC Project Manager

11. ABSTRACT *(200 words or less)*

The influence of gas venting on flame acceleration in an obstacle-laden tube has been investigated in the High-Temperature Combustion Facility (HTCF) at BNL. In these venting experiments, the flame was observed to accelerate very quickly in the first tube section before the first vent section. For lean hydrogen mixtures, after the first vent section, the flame velocity decayed to a velocity on the order of the laminar burning velocity. For more sensitive mixtures, the flame reached a quasi-steady flame velocity similar to flame propagation in the choking regime observed in tests without venting. For all initial temperatures, the lean limit for significant flame acceleration (i.e., choking regime limit) with venting increased over the nonventing case by an average of 2 percent hydrogen. In the choking regime, the flame was observed to accelerate in the tube section to a maximum velocity close to the speed of sound in the products and then decelerate across the vent section. At the limited temperatures tested where DDT was observed, the minimum hydrogen concentration required for transition to detonation increased with venting present as compared to without venting. In all cases, after a certain propagation distance, the detonation wave failed due to local venting effects and continued to propagate at a velocity characteristic of the choking regime.

12 KEY WORDS/DESCRIPTORS *(List words or phrases that will assist researchers in locating the report.)*

Hydrogen Combustion, Hydrogen - Explosions, Experimental Data, Flame Acceleration, Flame Propagation, Ignition, High-Temperature Combustion, High-Speed Combustion, Temperature Dependence, Venting

13. AVAILABILITY STATEMENT

Unlimited

14. SECURITY CLASSIFICATION

(This Page) Unclassified

(This Report) Unclassified

15. NUMBER OF PAGES

16. PRICE

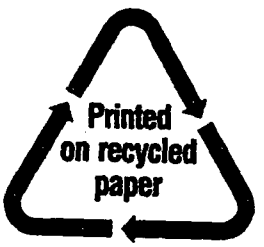

Federal Recycling Program